

SLAC-PUB-1338  
(T/E)  
November 1973

DEEP INELASTIC SCATTERING AND FINAL STATE HADRONS\*

Frederick J. Gilman  
Stanford Linear Accelerator Center  
Stanford University, Stanford, Calif. 94305

Lectures presented at the  
Summer Institute on Particle Interactions at Very High Energies  
Louvain, Belgium  
August 13-24, 1973

---

\* Work supported by the U. S. Atomic Energy Commission.

## I. Introduction

In the period of two years since the last Summer Institute at Louvain, the subject of deep inelastic scattering has continued to attract the attention of a sizeable proportion of both experimental and theoretical high energy physicists. During that time our experimental knowledge has not only increased in terms of further measurements with greater accuracy over the previously explored kinematical range, but access to two new areas has opened. These are inelastic muon and neutrino scattering experiments at NAL energies and electron-positron annihilation into hadrons at center-of-mass energies above 3 GeV. Furthermore, the scanty information available two years ago on final state hadrons has now been remedied by many experiments which, taken together, give a fairly complete picture of the nature of the final state hadrons in electroproduction for moderate virtual photon energies and momentum transfers.

We shall begin with several lectures reviewing what one expects from the quark light cone algebra, or more particularly, its concrete realization in terms of the quark parton model, for the behavior of deep inelastic electron-nucleon, neutrino-nucleon, and antineutrino-nucleon scattering and for electron-positron annihilation into hadrons. The most recent experimental data from SLAC, NAL and CEA is compared with our theoretical expectations and found to form a very simple consistent picture, with the possible exception of the results for  $\sigma(e^+e^- \rightarrow \text{hadrons})$ .

In the lecture following that, we discuss some of the salient pieces of experimental information that have been collected so far on the final hadrons in inelastic electron scattering. This sets the stage for the last lecture in which we discuss some of the theoretical ideas which have been put forth on this subject and classify them in the framework of a rather general analysis of the various regions of rapidity possible for the final hadron.

## II. Deep Inelastic Scattering and Annihilation

### A. Inelastic Electron-Nucleon Scattering

For inelastic electron scattering, the diagram of interest<sup>1,2</sup> is indicated in Fig. 1, where  $k$  and  $k'$  are the initial and final electron four-momenta,  $q$  is the four-momentum transfer carried by the virtual photon, and  $p$  is the target nucleon's four-momentum. The final hadronic state  $n$  then has four-momentum  $p_n = p+q$  and invariant mass squared  $W^2 = -(p+q)^2$ . In the laboratory frame (initial nucleon at rest) with  $E$  and  $E'$  the energies of the initial and final electrons, the Lorentz scalar variable

$$\nu = -p \cdot q / M_N = E - E' \quad (1)$$

is the virtual photon's energy, and the invariant momentum transfer squared is

$$q^2 = 4EE' \sin^2 \theta / 2 \quad (2)$$

where  $\theta$  is the scattering angle and the electron mass has been neglected compared to its energy. Knowing  $\nu$  and  $q^2$  from measuring the incident and scattered electron, the invariant mass  $W$  of the final hadrons is fixed by

$$W^2 = 2M_N \nu + M_N^2 - q^2. \quad (3)$$

The S-matrix element for the process in Fig. 1 may be written using the rules of quantum electrodynamics at the photon-electron vertex as

$$\begin{aligned} S_{fi} = & \delta_{fi} + (2\pi)^4 i \delta^{(4)}(p_n + k' - p - k) \sqrt{\frac{m_e^2}{EE'}} (-\bar{e}u(k') i \gamma_\mu u(k)) \\ & \times (\delta_{\mu\nu} / q^2) \langle p_n | J_\nu(0) | p \rangle, \end{aligned} \quad (4)$$

where

$$J_\nu = e \left( V_\mu^3 + \frac{1}{\sqrt{3}} V_\mu^8 \right) \quad (5)$$

is the (hadronic) electromagnetic current operator and  $V_\mu^\alpha(x)$  is the vector current density. Averaging over initial and summing over final electron and nucleon spins, we are led to an expression for the double differential cross section in the laboratory for detection of only the final electron of the form

$$\frac{d^2\sigma}{d\Omega'dE'} = \frac{1}{(2\pi)^2} \left(\frac{E'}{E}\right) \left(\frac{e^2}{q^2}\right)^2 L_{\mu\nu} W_{\mu\nu}, \quad (6)$$

where the factor  $L_{\mu\nu}$  arises from the trace of the gamma matrices due to the electron (neglecting the electron mass),

$$L_{\mu\nu} = \frac{1}{2} \left[ k_\mu k'_\nu + k'_\mu k_\nu + \left(\frac{q^2}{2}\right) \delta_{\mu\nu} \right], \quad (7)$$

and the structure of the nucleon is summarized in

$$\begin{aligned} W_{\mu\nu} &= \frac{1}{2} \sum_{\text{nucleon spin}} \sum_n \left(\frac{1}{e}\right) \langle p | J_\mu(0) | n \rangle \langle n | J_\nu(0) | p \rangle \\ &\times (2\pi)^3 \delta^{(4)}(p_n - p - q) \\ &= \frac{1}{2} \sum_{\text{nucleon spin}} \frac{1}{(2\pi e^2)} \int d^4x e^{-iq \cdot x} \langle p | [J_\mu(x), J_\nu(0)] | p \rangle \\ &= \frac{1}{2} \sum_{\text{nucleon spin}} \left(\frac{1}{2\pi}\right) \int d^4x e^{-iq \cdot x} \langle p | [V_\mu(x), V_\nu(0)] | p \rangle, \quad (8) \end{aligned}$$

where the second term in the commutator is zero by energy conservation for  $\nu > 0$ .

By Lorentz and gauge invariance the tensor  $W_{\mu\nu}$  may be written as

$$\begin{aligned} W_{\mu\nu} &= W_1(\nu, q^2) (\delta_{\mu\nu} - q_\mu q_\nu / q^2) \\ &+ W_2(\nu, q^2) (p_\mu - p \cdot q q_\mu / q^2) (p_\nu - p \cdot q q_\nu / q^2) / M_N^2. \quad (9) \end{aligned}$$

The quantity  $W_{\mu\nu}$  is just  $(1/4 \pi^2 \alpha)$  times the imaginary part of the Feynman amplitude for forward Compton scattering of virtual photons of mass<sup>2</sup> =  $-q^2$ . In terms of  $W_1$  and  $W_2$  the experimentally measured double differential cross section resulting from combining Eqs. (6), (7) and (9) is

$$\frac{d^2\sigma}{d\Omega' dE'} = \frac{4\alpha^2 E'^2}{q^4} \left[ 2W_1(\nu, q^2) \sin^2 \theta/2 + W_2(\nu, q^2) \cos^2 \theta/2 \right], \quad (10)$$

so that the structure functions  $W_1$  and  $W_2$ , as they depend on  $\nu$  and  $q^2$ , summarize the results of inelastic electron-nucleon scattering.

Now suppose that  $\nu$  and  $q^2$  are large, with  $\nu/q^2$  fixed. In the expression, Eq. (8), for  $W_{\mu\nu}$  in terms of the Fourier transform of a commutator of two currents the exponential is

$$\begin{aligned} e^{-iq \cdot x} &= e^{-i(q_z z - q_0 t)} = e^{-i(\sqrt{q^2 + \nu^2} z - \nu t)} \\ &\simeq e^{-i\nu(z-t)} e^{-i(q^2/2\nu)z} \end{aligned} \quad (11)$$

in this domain of  $\nu$  and  $q^2$  with  $\vec{q}$  in the  $z$  direction. In order that the argument of the exponential not become large and produce cancelling oscillations of the integrand, the region of integration in configuration space must satisfy

$$\begin{aligned} z - t &\lesssim 0(1/\nu) \\ z &\lesssim 0(2\nu/q^2). \end{aligned} \quad (12)$$

Furthermore, since we want the commutator to be causal, it should vanish unless

$$x^2 = x_{\perp}^2 + z^2 - t^2 \leq 0, \quad (13)$$

which together with Eqs. (12) yields

$$x_{\perp}^2 \leq (t-z)(t+z) \lesssim 0(1/q^2). \quad (14)$$

Therefore, the important region of integration over the current commutator is  $x^2 = x_\mu x_\mu \simeq 0$ , i. e., along the light-cone.<sup>3</sup>

To gain theoretical insight into the commutator of two currents on the light-cone we turn to the quark model and abstract certain properties, particularly algebraic ones, of such commutators from the free field case. In the free quark model one finds<sup>4,5</sup>

$$\begin{aligned}
\left[ V_\mu^\alpha(x), V_\nu^\beta(0) \right] \underset{x^2 \rightarrow 0}{\sim} & \left\{ i f^{\alpha\beta\gamma} \left[ \left( V_\nu^\gamma(x,0) + V_\nu^\gamma(0,x) \right) \delta_{\mu\lambda} \right. \right. \\
& + \left( V_\mu^\gamma(x,0) + V_\mu^\gamma(0,x) \right) \delta_{\nu\lambda} \\
& - \left. \left( V_\lambda^\gamma(x,0) + V_\lambda^\gamma(0,x) \right) \delta_{\mu\nu} \right. \\
& + i \epsilon_{\mu\nu\lambda\sigma} \left( A_\sigma^\gamma(x,0) - A_\sigma^\gamma(0,x) \right) \left. \right] \\
& + d^{\alpha\beta\gamma} \left[ \left( V_\nu^\gamma(x,0) - V_\nu^\gamma(0,x) \right) \delta_{\mu\lambda} \right. \\
& + \left( V_\mu^\gamma(x,0) - V_\mu^\gamma(0,x) \right) \delta_{\nu\lambda} \\
& - \left. \left( V_\lambda^\gamma(x,0) - V_\lambda^\gamma(0,x) \right) \delta_{\mu\nu} \right. \\
& - \left. \left. i \epsilon_{\mu\nu\rho\sigma} \left( A_\sigma^\gamma(x,0) + A_\sigma^\gamma(0,x) \right) \right] \right\} \\
& \frac{1}{4\pi} \partial_\lambda \left[ \epsilon(x_0) \delta(x^2) \right], \tag{15}
\end{aligned}$$

where  $V_\mu^\alpha(x)$  and  $A_\mu^\alpha(x)$  are the vector and axial vector currents and

$$V_\mu^\alpha(x,0) = : \bar{\psi}(x) (\lambda^\alpha / 2) i \gamma_\mu \psi(0) :$$

and

$$A_\mu^\alpha(x,0) = : \bar{\psi}(x) (\lambda^\alpha / 2) i \gamma_\mu \gamma_5 \psi(0) : \tag{16}$$

are bilocal operators defined so that

$$V_{\mu}^{\alpha}(x, x) = V_{\mu}^{\alpha}(x) \quad (17a)$$

and

$$A_{\mu}^{\alpha}(x, x) = A_{\mu}^{\alpha}(x) . \quad (17b)$$

All the SU(3) properties are summarized by the SU(3) structure constants  $f^{\alpha\beta\gamma}$  and  $d^{\alpha\beta\gamma}$ . In fact, if we specialize to the time components of the currents and go to the tip of the light cone ( $x_0 = 0$ ) then we recover the old equal time algebra of Gell-Mann.<sup>6</sup>

An important property of Eq. (15) is that it factorizes into a product of a  $c$ -number singularity which contains no masses or other dimensional parameters and a bilocal operator which carries the SU(3) indices. When Eq. (15), as the leading light-cone singularity in the limit  $\nu, q^2 \rightarrow \infty$ , is inserted back in Eq. (8) for  $W_{\mu\nu}$ , it is seen that Fourier transforms of matrix elements of the bilocal turn out to be the structure functions and that  $W_1$  and  $\nu W_2$  scale,<sup>7</sup> i.e., are functions of  $\omega = 2M_N \nu/q^2 = -2p \cdot q/q^2$ . Because of the structure of the tensor indices in Eq. (15), one also obtains the relation:

$$\frac{2M_N}{\omega} W_1(\omega) = \nu W_2(\omega) , \quad (18)$$

which corresponds to the vanishing of the longitudinal relative to transverse photon-nucleon total cross sections ( $\sigma_L/\sigma_T = 0$ ) in the indicated limit.

Another, more mundane, way to see that it is  $\nu W_2$  and  $W_1$  which should scale if there is no dimensionless parameter or scale in the virtual photon-nucleon interaction is to rewrite the double differential cross section in Eq. (10) in terms of the dimensionless variables

$$x = \frac{1}{\omega} = -q^2/2p \cdot q = q^2/2M_N \nu \quad (19)$$

and

$$y = \nu/E = p \cdot q/p \cdot k . \quad (20)$$

Then in the high energy regime where  $\nu$  and  $q^2$  are both large, we can write

$$\frac{d^2\sigma}{dx dy} = \left( \frac{4\pi\alpha^2}{q^4} \right) (2M_N E) \left[ (1-y) \nu W_2 + \frac{1}{2} y^2 2M_N x W_1 \right] , \quad (21)$$

where terms of order  $M_N/\nu$  and  $M_N/E$  have been neglected. The factor  $(4\pi\alpha^2/q^4)$  is just the elastic electron scattering cross section for a point particle.

We see immediately that if the quantity in brackets, which involves the photon-nucleon interaction, is not to depend on some internal scale, then  $\nu W_2$  and  $2M_N x W_1$  should only depend on a dimensionless variable involving the photon-nucleon vertex, i. e., they should depend on  $x = -q^2/2p \cdot q = 1/\omega$ .

The absence of any scale in the interaction of a virtual photon with a nucleon is realized explicitly in the parton model,<sup>8,9</sup> which might also be regarded as a concrete representation of the light cone algebra. In the parton model one regards the nucleon as composed of point constituents. In an infinite momentum frame, each type (i) of parton, with charge  $Q_i$  (in units of e), is taken to have a distribution  $f_i(x)$  in the fractional longitudinal momentum  $x = p_z^{(\text{parton})}/p_z^{(\text{nucleon})}$ . A straightforward calculation then shows that for spin 1/2 partons

$$\nu W_2 = \sum_i Q_i^2 x f_i(x) = 2M_N x W_1(x) , \quad (22)$$

where  $x$  is both the fractional longitudinal momentum of the struck parton and the value of the scaling variable  $q^2/2M_N\nu$ . Taking the partons to be quarks (and more generally, also antiquarks) one has a concrete representation of the quark light cone algebra. As with any particular representation of a given algebra, certain results may hold which do not follow necessarily in the general case.

The scaling behavior exhibited by the data<sup>10, 11</sup> outside the region of prominent resonances for  $\nu W_2$  and  $2M_N W_1$  is shown in Fig. 2. There the values of the structure functions are plotted versus  $\omega' = 1 + W^2/q^2 = \omega + M_N^2/q^2$ , which is the same as  $\omega$  in the limit  $\nu, q^2 \rightarrow \infty$ . Clearly values of  $\nu W_2$  and  $2M_N W_1$  at the same  $\omega'$  but different  $q^2$  coincide, i.e.,  $\nu W_2$  and  $2M_N W_1$  for the proton are functions of  $\omega'$  to within the accuracy of the data for  $q^2 > 1 \text{ GeV}^2$  and  $1 < \omega' < 10$ .

The validity of the relation  $\nu W_2 = 2M_N x W_1$  as  $\nu, q^2 \rightarrow \infty$  is more clearly examined in terms of the quantity  $R = \sigma_L/\sigma_T$ , which should then vanish as  $\nu, q^2 \rightarrow \infty$  at fixed  $\omega$ . A previous global average of  $R$  for the proton gave the value<sup>11</sup>  $R_p = 0.18 \pm 0.10$ . Newer data, but over essentially the same kinematic range, has recently been analyzed and yields<sup>12</sup> a global average in agreement with this. More interestingly, there is some indication<sup>12</sup> that  $R_p$  is vanishing as  $1/\nu$  for fixed values of  $\omega \lesssim 5$ . The analysis of the deuteron data taken in the same experiment shows<sup>12</sup> that  $R_p = R_d = R_n$  to within the statistical errors of the measurement ( $\pm 0.04$ ).

The ratio of neutron to proton inelastic cross sections, as extracted from deuterium data, shows consistency with the neutron structure functions scaling also.<sup>13, 14</sup> The ratio of n/p decreases from values near unity at small  $x$  (and large  $\omega = 1/x$ ) to values<sup>14</sup> definitely below 1/2 for  $x > 0.65$ .

For values of  $x$  near one, where it appears that the n/p ratio is the smallest, one could hope to challenge the bounds from the quark light-cone algebra:<sup>15</sup>

$$\frac{1}{4} \leq n/p \leq 4 .$$

Although present data extends to  $x \simeq 0.8$  and doesn't indicate any violation of the lower bound, experiments are under way to investigate the region near  $x = 1$  in considerable detail.

Also of interest is the region of small  $x$  or large  $\omega$  where the  $n/p$  ratio is expected to eventually approach unity on the basis of the dominance of the Pommeranchuk singularity in the photon-nucleon amplitude at large values of  $\omega$ . Some recent data<sup>16</sup> on this ratio is shown in Fig. 3 where it is seen that even for values of  $\omega$  between 10 and 20 the value of  $n/p$  is still only  $\sim 0.85$  and only slowly approaching unity. This bears directly on the convergence of the sum rule<sup>17</sup>

$$\int_1^{\infty} \frac{d\omega}{\omega} \left[ \nu W_{2p}(\omega) - \nu W_{2n}(\omega) \right] = \frac{1}{3} . \quad (23)$$

This can be derived in parton models where the nucleon is composed of three "valence" quarks plus an isoscalar "sea" of  $q\bar{q}$  pairs (plus neutrals), or it can be derived using exchange degeneracy arguments,<sup>18</sup> but it does not follow generally from the quark light cone algebra. Earlier evaluations of the sum rule using then existing data and Regge extrapolations for  $\nu W_{2p}(\omega) - \nu W_{2n}(\omega)$  as  $\omega \rightarrow \infty$  gave the estimate  $0.19 \pm 0.06$  for the left hand side.<sup>13</sup> The data shown in Fig. 3, however, gives<sup>16</sup>

$$\int_1^{20} \frac{d\omega}{\omega} \left[ \nu W_{2p}(\omega) - \nu W_{2n}(\omega) \right] = 0.18 \pm 0.04 , \quad (24)$$

and a rough estimate of the contribution from  $\omega = 20$  to  $\infty$  is 0.09. There is no longer an experimental basis for worrying about the sum rule's validity.

#### B. Inelastic Neutrino- and Antineutrino-Nucleon Scattering

The extension of our discussion to inelastic neutrino and antineutrino scattering is easily made. Again neglecting lepton masses and averaging over nucleon

spins, the double differential cross section is<sup>19</sup>

$$\frac{d^2\sigma(\nu/\bar{\nu})}{d\Omega'dE'} = \frac{G^2 E'^2}{2\pi^2} \left[ 2 \sin^2\theta/2 W_1^{(\nu/\nu)}(\nu, q^2) + \cos^2\theta/2 W_2^{(\nu/\bar{\nu})}(\nu, q^2) \mp \frac{E+E'}{M_N} \sin^2\theta/2 W_3^{(\nu/\bar{\nu})}(\nu, q^2) \right], \quad (25)$$

with  $G \simeq 1.0 \times 10^{-5}/M_N$  the weak coupling constant. In the high energy limit, using the same variables  $x$  and  $y$  in Eqs. (19) and (20) as before, this becomes

$$\frac{d^2\sigma(\nu/\bar{\nu})}{dx dy} = \left( \frac{G^2 M_N E}{\pi} \right) \left[ (1-y) \nu W_2 + \frac{y^2}{2} (2M_N x) W_1 \mp y \left( 1 - \frac{1}{2}y \right) x \nu W_3 \right]. \quad (26)$$

The structure functions  $W_1$  and  $W_2$  now involve Fourier transforms of both vector-vector and axial vector-axial vector current commutators, while the new structure function  $W_3$  involves only vector-axial vector commutators. Neglecting strangeness changing currents, the restriction of the weak, strangeness non-changing current to have isospin one implies that

$$\begin{aligned} W_i^{\nu p} &= W_i^{\bar{\nu} n} \\ W_i^{\nu n} &= W_i^{\bar{\nu} p} \end{aligned} \quad (27)$$

The quark light cone algebra in Eq. (15) is also simply extended<sup>4,5</sup> to include commutators of two axial-vector currents or a vector and axial-vector current. As an immediate consequence it follows that  $2M_N x W_1$ ,  $\nu W_2$ , and  $\nu W_3$  should scale, as can also be seen directly from Eq. (26) using the argument that if the weak current-nucleon interaction doesn't depend on parameters with dimensions, then the quantity in brackets on the right-hand side should involve structure functions in combinations which only depend on the dimensionless quantity  $x$ . Scaling of  $W_1 = F_1(x)$ ,  $\nu W_2 = F_2(x)$ , and  $\nu W_3 = F_3(x)$  implies

on integrating Eq. (26) first over  $y$  and then over  $x$  that

$$\sigma_{\text{TOT}}^{(\nu/\bar{\nu})} = \frac{G^2 M_N E}{\pi} \int_0^1 dx \left[ \frac{F_2(x)}{2} + \frac{2M_N x F_1(x)}{6} \mp \frac{x F_3(x)}{6} \right], \quad (28)$$

i. e., that the total neutrino or antineutrino cross section rises linearly with the incident beam energy,  $E$ .

From the quark light cone algebra we have furthermore that<sup>4, 5, 19</sup>

$$2M_N x F_1(x) = F_2(x), \quad (29)$$

and the local relation between inelastic electron and neutrino scattering:

$$6 \left[ F_2^{\text{ep}}(x) - F_2^{\text{en}}(x) \right] = x \left[ F_3^{\nu\text{p}}(x) - F_3^{\nu\text{n}}(x) \right]. \quad (30)$$

Various sum rules follow as well, including

$$\int_0^1 \frac{dx}{x} \left[ F_2^{\nu\text{n}}(x) - F_2^{\nu\text{p}}(x) \right] = 2, \quad (31)$$

the Adler sum rule,<sup>20</sup> which actually is supposed to hold for all  $q^2$ , and the sum rule<sup>21</sup>

$$\int_0^1 dx \left[ F_3^{\nu\text{p}}(x) + F_3^{\nu\text{n}}(x) \right] = -6. \quad (32)$$

In a parton model with only fermion constituents which interact with the current (no antifermions) one has as well that

$$F_2(x) = 2M_N x F_1(x) = -x F_3(x), \quad (33)$$

i. e., maximal V-A interference.

The simplest quantity with which to compare theory and experiment is the total cross section summed over neutrino and antineutrino beams. From Eq. (28) we find that the  $F_3$  term cancels in the sum and using  $F_2(x) = 2M_N x F_1(x)$

yields

$$\sigma_{\text{TOT}}^{\nu N}(\mathbf{E}) + \sigma_{\text{TOT}}^{\bar{\nu} N}(\mathbf{E}) = \frac{G^2 M_N E}{\pi} \frac{4}{3} \left[ \frac{1}{2} \int_0^1 dx \left( F_2^{\nu N}(x) + F_2^{\bar{\nu} N}(x) \right) \right]. \quad (34)$$

We write  $\nu N$  ( $\bar{\nu} N$ ) to denote an average over neutrino (antineutrino) cross sections on protons and neutrons. Of course,

$$F_2^{\nu N}(x) = \frac{1}{2} \left( F_2^{\nu p}(x) + F_2^{\nu n}(x) \right) = \frac{1}{2} \left( F_2^{\bar{\nu} p}(x) + F_2^{\bar{\nu} n}(x) \right) = F_2^{\bar{\nu} n}(x). \quad (35)$$

The data from the Gargamelle experiment<sup>22</sup> are quite consistent with a linear rise with  $\mathbf{E}$  of  $\sigma_{\text{TOT}}(\mathbf{E})$  for both neutrinos and antineutrinos. The coefficients of  $G^2 M_N E / \pi$  yield<sup>22</sup>

$$\frac{1}{2} \int_0^1 dx \left( F_2^{\nu N}(x) + F_2^{\bar{\nu} N}(x) \right) = 0.47 \pm 0.07. \quad (36)$$

To relate this to electron scattering we must make some additional assumption beyond just the light cone algebra. We assume that in the  $x$  region which gives the most important contribution to  $\int_0^1 dx F_2(x)$ , one has only quark partons (no antiquarks). As we will see in a moment there is independent support for this from the ratio  $\sigma_{\text{TOT}}^{\bar{\nu} N} / \sigma_{\text{TOT}}^{\nu N}$ . With no antiquarks, one has the relation<sup>23</sup>

$$\frac{1}{2} \left( F_2^{\nu N}(x) + F_2^{\bar{\nu} N}(x) \right) = \frac{18}{5} \left( \frac{1}{2} \right) \left( F_2^{\text{ep}}(x) + F_2^{\text{en}}(x) \right), \quad (37)$$

which together with the result from SLAC data (with a minor extrapolation)<sup>10, 11</sup>

$$\frac{1}{2} \int_0^1 dx \left( F_2^{\text{ep}}(x) + F_2^{\text{en}}(x) \right) = 0.15 \pm 0.01, \quad (38)$$

predicts that

$$\frac{1}{2} \int_0^1 dx \left( F_2^{\nu N}(x) + F_2^{\bar{\nu} N}(x) \right) = 0.54 \pm 0.04. \quad (39)$$

The agreement with the direct measurement, Eq. (36), is obviously very good.<sup>24</sup>

Now let us return to  $\sigma_{\text{TOT}}(E)$  for neutrinos and antineutrinos separately.

Rewriting Eq. (28) we have

$$\sigma_{\text{TOT}}^{(\nu/\bar{\nu})}(E) = \frac{G^2 ME}{\pi} \int_0^1 dx F_2(x) \left[ \frac{1}{2} + \frac{1}{6} \pm \frac{B}{3} \right], \quad (40)$$

and therefore

$$\sigma_{\text{TOT}}^{\bar{\nu}N} / \sigma_{\text{TOT}}^{\nu N} = (2 - B)/(2 + B) \quad (41)$$

where

$$B = - \int_0^1 dx xF_3(x) / \int_0^1 dx F_2(x) . \quad (42)$$

Purely from kinematic inequalities  $|xF_3| \leq F_2(x)$  or  $|B| \leq 1$ . The extreme values of B correspond to maximal V-A interference and are met for purely fermion partons ( $B = +1$ ) or purely antifermion partons ( $B = -1$ ). The experimental value of<sup>22</sup>

$$\sigma_{\text{TOT}}^{\bar{\nu}N} / \sigma_{\text{TOT}}^{\nu N} = 0.38 \pm 0.02 \quad (43)$$

gives<sup>25</sup>

$$B = 0.90 \pm 0.04 , \quad (44)$$

and indicates almost purely fermion constituents in the region accessible to the Gargamelle experiment. Everything is quite consistent with the quark light cone algebra or the even more restrictive quark parton model with only a small component of antiquarks.

In the past few months the first data on inelastic neutrino scattering at NAL have been reported. The Caltech experiment<sup>26</sup> uses a "narrow band" beam with neutrinos of average energies of 50 and 145 GeV arising from decays of 160 GeV

pions and kaons, respectively. While there are only 112 neutrino events from a steel target reported, they already allow some tentative conclusions.<sup>26</sup>

If one assumes  $2M_N x F_1(x) = F_2(x) = -xF_3(x)$ , then Eq. (26) becomes

$$\frac{d^2 \sigma^{\nu N}}{dx dy} = \frac{G^2 M_N E}{\pi} F_2^{\nu N}(x) \quad (45)$$

which is independent of  $y$ . Within large errors, the data are consistent with  $y$  independence. Although the flux is not known accurately, one can integrate over  $y$  and compare the shape of  $d\sigma^{\nu N}/dx$  with what is seen at Gargamelle, or the better determined  $F_2^{ep} + F_2^{en} \simeq F_2^{ed}$ . This is shown in Fig. 4, with consistency seen between the  $x$  distribution measured with high energy neutrinos and that measured with electrons at SLAC.

A more stringent test of scaling is provided by the quantity

$$\langle q^2 \rangle = \langle xy 2M_N E \rangle = 2M_N E \langle xy \rangle, \quad (46)$$

where

$$\langle f(x, y) \rangle = \frac{\int_0^1 \int_0^1 dx dy f(x, y) \frac{d^2 \sigma}{dx dy}}{\int_0^1 \int_0^1 dx dy \frac{d^2 \sigma}{dx dy}}. \quad (47)$$

$\langle q^2 \rangle$  should therefore rise linearly with  $E$  if there is scaling. The comparison with the results from the Caltech experiment for  $\langle q^2 \rangle$  are shown in Fig. 5, where the curves are computed using the acceptance of the apparatus and assuming

$$\frac{d^2 \sigma}{dx dy} = \frac{G^2 M_N E}{\pi} \frac{F_2(x)}{(1 + q^2/\Lambda^2)^2} \quad (48)$$

Again the data are consistent with  $\Lambda = \infty$ , i.e., scaling. Note the large values of  $\langle q^2 \rangle$  seen at NAL energies — in itself an indication of a "point-like" interaction.

A second experiment with a "broad band" beam of mean energy  $\sim 50$  GeV has been carried out by a Harvard-Pennsylvania-Wisconsin collaboration.<sup>27, 28</sup>

With about 300 neutrino and antineutrino events they are able to state that<sup>28</sup>  $\sigma_{\text{TOT}}^{\nu N} + \sigma_{\text{TOT}}^{\bar{\nu} N}$  is very roughly ten times larger at a mean energy of 50 GeV than it is at 5 GeV in the Gargamelle experiment, just as expected from scaling (Eq. (28)). The ratio  $\sigma^{\bar{\nu} N} / \sigma^{\nu N}$  lies between 1/3 and 1/2 and is therefore consistent with the Gargamelle result of  $0.38 \pm 0.02$ . Note that if

$$v = xy = 2E' \sin^2 \theta / 2M_N, \quad (49)$$

then<sup>29</sup>  $\frac{1}{N} \frac{dN}{dv}$  is independent of flux and is a function of  $v$  alone if the structure functions scale. Analysis of their data shows that<sup>28</sup> both their neutrino and antineutrino data are consistent with scaling, and more particularly, with the  $\frac{1}{N} \frac{dN}{dv}$  curves calculated on the basis of the SLAC electron scattering data and the quark parton model.

Thus both high energy neutrino experiments seem to show that while we have increased the beam energies by an order of magnitude or better, nothing striking has changed from what was learned with Gargamelle. Everything seems remarkably consistent with the rather simple picture of scaling embodied in the quark light cone algebra and the quark parton model.

### C. Electron-Positron Annihilation into Hadrons

There is one major indication of trouble with this simple picture: electron-positron annihilation into hadrons via one photon. The cross section for  $e^+ e^- \rightarrow \text{hadrons}$  is directly proportional to  $\int d^4x e^{-iq \cdot x} \langle 0 | [J_\mu(x), J_\nu(0)] | 0 \rangle$ . As a result, in the  $e^+ e^-$  center-of-mass where  $\vec{q} = 0$  and  $q_0 = \sqrt{|q^2|}$ , the limit  $q_0 \rightarrow \infty$  or  $|q^2| \rightarrow \infty$  implies that  $x_0 \approx 0$  and  $\vec{x} \approx 0$ , i.e., the tip of the light cone, is the important region of integration in that limit. As a result, assuming the

quark model also gives the disconnected part of the commutator on the light cone, one finds

$$\sigma(e^+e^- \rightarrow \text{hadrons}) = \left( \frac{4\pi\alpha^2}{3|q^2|} \right) \sum_i Q_i^2, \quad (50)$$

where the sum is over the charged quark pairs creatable by the electromagnetic current. The quantity  $(4\pi\alpha^2/3|q^2|)$  is just the cross section for  $e^+e^- \rightarrow \mu^+\mu^-$ . Three quark constituents with charges  $2/3$ ,  $-1/3$ , and  $-1/3$  yield  $\sum_i Q_i^2 = 2/3$ , while colored quarks<sup>30</sup> give  $\sum_i Q_i^2 = 2$ , and the Han-Nambu integrally charged quark scheme<sup>31</sup> has  $\sum_i Q_i^2 = 4$ . The present experimental situation is seen<sup>32</sup> in Fig. 6 including the most recent CEA results<sup>33</sup> for  $\sigma(e^+e^- \rightarrow \text{hadrons})/\sigma(e^+e^- \rightarrow \mu^+\mu^-)$  of  $4.8 \pm 1.1$  and  $6.3 \pm 1.5$  at  $|q^2| = 16$  and  $25 \text{ GeV}^2$ , respectively.

The seeming disagreement with our expectations leads one to ask whether there is a breakdown in the scaling behavior,<sup>34</sup> i. e., whether  $\sigma(e^+e^- \rightarrow \text{hadrons})$  does not behave as  $1/q^2$  as  $|q^2| \rightarrow \infty$ . A careful reexamination of the electron and neutrino data is also called for, particularly to look for the behavior<sup>35</sup> of the moments  $\int_0^1 dx x^n F_2(x)$  as powers of  $(1/\ln q^2)$ , as suggested in asymptotically free gauge theories.<sup>36</sup> Most important experimentally, one awaits the results from SPEAR and DORIS on the magnitude of  $\sigma(e^+e^- \rightarrow \text{hadrons})$  at the same as well as still higher values of  $|q^2|$ .

### III. Some Experimental Results on Final State Hadrons in Inelastic Electron Scattering

#### A. Kinematical Considerations

Consider inelastic electron-nucleon scattering where a final hadron (four-momentum  $p'_\mu$ ) is detected. In such a process there are two planes: one determined by  $\vec{k}$  and  $\vec{k}'$  (the lepton plane), the other by  $\vec{q}$  and  $\vec{p}'$  (the hadron plane), with an angle  $\phi$  between their normals.

Rather than work with structure functions, it is more convenient at this point to consider the physics in terms of cross sections for a virtual photon incident on a nucleon. Recall from Section II that to calculate a cross section for inelastic electron-nucleon scattering we must evaluate a lepton trace,  $L_{\mu\nu}$ , which is essentially the virtual photon density matrix. If we take the direction of  $\vec{q}$  as a z-axis, with x-axis in the lepton plane (so that the positive x direction is toward the leptons) then  $L_{\mu\nu} = (1/2)(k_{\mu}k'_{\nu} + k'_{\mu}k_{\nu} + (q^2/2) \delta_{\mu\nu})$  can be written as

$$L_{\mu\nu} = \left(\frac{2}{1-\epsilon}\right) \left(\frac{q^2}{4}\right) \left\{ \begin{array}{c} \left( \begin{array}{c} \sqrt{\frac{1}{2}(1+\epsilon)} \\ 0 \\ -\sqrt{q^2\epsilon/\nu^2} \\ 0 \end{array} \right) \left( \begin{array}{c} \sqrt{\frac{1}{2}(1+\epsilon)} \\ 0 \\ -\sqrt{q^2\epsilon/\nu^2} \\ 0 \end{array} \right) + \left( \begin{array}{c} 0 \\ \sqrt{\frac{1}{2}(1-\epsilon)} \\ 0 \\ 0 \end{array} \right) \left( \begin{array}{c} 0 \\ \sqrt{\frac{1}{2}(1-\epsilon)} \\ 0 \\ 0 \end{array} \right) \end{array} \right\} \quad (51)$$

where

$$\epsilon = \frac{1}{1 + 2 \left( 1 + \left( \frac{\nu^2}{q^2} \right) \tan^2 \theta/2 \right)}, \quad (52)$$

We have subtracted multiples of  $q_{\mu}$  from the virtual photon polarization vector so as to make  $L_{\mu\nu} = 0$  when  $\mu$  or  $\nu = 4$ . As is seen from Eq. (52), the virtual photon is the incoherent sum of a piece with linear polarization in the x-z plane and a piece with linear polarization in the y-direction.

If  $\epsilon_{\mu}^{(\gamma)} f_{\mu}$  is the amplitude for

$$" \gamma(q) " + N(p) \rightarrow \text{hadron}'(p') + \dots ,$$

with the property

$$q_\mu f_\mu = 0 \quad , \quad (53)$$

then from Eq. (51) we have that

$$\begin{aligned} \frac{d\sigma}{d^3p'} &\propto \left| \sqrt{\frac{1}{2}(1+\epsilon)} f_x - \sqrt{q^2 \epsilon / \nu^2} f_z \right|^2 + \left| \sqrt{\frac{1}{2}(1-\epsilon)} f_y \right|^2 \\ &\propto \frac{1}{2} (|f_x|^2 + |f_y|^2) \\ &+ \frac{\epsilon}{2} (|f_x|^2 - |f_y|^2) \\ &+ \epsilon (q^2 |f_z|^2 / \nu^2) \\ &- \sqrt{\frac{1}{2} \epsilon (1+\epsilon)} 2 \operatorname{Re} (f_x \sqrt{q^2 / \nu^2} f_z^*) \quad . \end{aligned} \quad (54)$$

The four terms in Eq. (54) are in the form of the standard equation for, e.g., " $\gamma$ " + p  $\rightarrow$   $\pi^+$  + n, where they are often labelled<sup>37</sup>  $d\sigma_U/dt$ ,  $d\sigma_P/dt$ ,  $d\sigma_L/dt$ , and  $d\sigma_I/dt$  respectively, after their  $\phi$  dependence is explicitly exhibited. This  $\phi$  dependence is easily read off if  $f_x$ ,  $f_y$  and  $f_z$  are rewritten in terms of helicity amplitudes (of the virtual photon). The four terms behave respectively as constant,  $\cos 2\phi$ , constant, and  $\cos \phi$ .

With the use of a polarized lepton beam it becomes possible to measure one more quantity,  $\operatorname{Im}(f_y f_z^*)$ . The set of four quantities in Eq. (54), plus this last one, gives all the possible physical information on  $f_\mu$ .

## B. An Exclusive Channel: Rho Electroproduction

Rather than attempt to cover all the information gathered in the past few years on final state hadrons, we will instead concentrate on a few selected topics to show some of the important features. We begin with the electroproduction of rho mesons which has received attention in a number of

experiments and is therefore a well-studied example of a diffractive process out to values of  $q^2$  of  $\sim 1.5 \text{ GeV}^2$ .

While  $\gamma p \rightarrow \rho^0 p$  has the largest cross section ( $\sim 11\%$  of  $\sigma_T(\gamma p)$ ) of any single channel in photoproduction, as  $q^2$  increases from zero (becomes more space-like), the integrated cross section for this process decreases as a proportion of the total cross section. The results of a particular experiment<sup>38</sup> are shown in Fig. 7, where  $\langle \nu \rangle \simeq 10 \text{ GeV}$ . Similar results have been obtained at Cornell,<sup>39</sup> DESY,<sup>40</sup> and SLAC.<sup>41</sup> It also appears that the processes " $\gamma$ " $p \rightarrow \omega p$  and " $\gamma p$ " $\rightarrow \phi p$  have a similar behavior,<sup>38,40,41</sup> although " $\gamma$ " $p \rightarrow \omega p$  perhaps falls off a little slower with  $q^2$  at low energies, where pion exchange is an important contributor to the amplitude.

At the same time that the integrated cross section is falling, the angular distribution seems to be getting broader. While the subject of some controversy for a time, a consistent "antishrinkage" of the diffraction peak as  $q^2$  increases is seen in several different experiments. What remains to be settled is the exact magnitude of the change and whether it depends on any other variable than  $q^2$  in a significant way.

The spin density matrix element of the rho can be determined from its two pion decay, while that of the virtual photon is completely known from the incident and final leptons momenta (see Eq. (51)). While all the possible joint density matrix elements have not been determined in any experiment so far, all measured elements are consistent with the hypothesis that s-channel helicity is conserved in the scattering of the photon into a rho, as in photoproduction.<sup>42</sup> The presence of both longitudinal and transverse virtual photons in electroproduction allows one to show experimentally that the longitudinal and transverse (helicity 0 and  $\pm 1$ , respectively) rho production amplitudes have exactly the same phase within

errors.<sup>38,40,41</sup> This of course implies there is non-negligible production of rhos in both longitudinal and transverse states. In fact, it appears that<sup>38,40,41</sup> longitudinal rhos are  $\sim 40\%$  of transverse rhos in the cross section at  $q^2 = 0.5$  to  $1.0 \text{ GeV}^2$ .

Therefore, rho electroproduction behaves differently than the total cross section. Up to this time, it does not appear that any particular channel imitates the  $q^2$  behavior of the total cross section. If we are searching for consequences of a possible hadron substructure, we must look instead at inclusive reactions.

### C. An Inclusive Reaction: Production of Pions

As in hadronic processes, it is conventional to classify produced hadrons according to either their rapidity,

$$y = \frac{1}{2} \ln \frac{E' + p'_{\parallel}}{E' - p'_{\parallel}} \quad (55)$$

or according to their value of the Feynman variable  $x = p'_{\parallel} / p'_{\parallel}^{\text{max}}$ , where  $p'_{\parallel}$  is the longitudinal momentum along the beam direction in the center of mass. Particles with finite values of  $x > 0$  ( $x < 0$ ) are said to be in the beam (target) fragmentation region, while those with  $x \approx 0$  are in the central region.

Naturally, one expects at sufficiently high energy that hadrons found in the target fragmentation region or in the central region should not depend on the characteristics of the beam. This has been amply confirmed in various hadronic experiments, but is also seen with real or virtual photon beams.

For example, with a polarized photon beam, one finds no  $\phi$  dependence of the direction of produced pions in either the nucleon fragmentation or central regions. But, particularly in a DESY experiment,<sup>43</sup> significant  $\cos\phi$  and  $\cos 2\phi$  terms are seen in the virtual photon fragmentation region.

Another example is to be found in the transverse momentum ( $p_{\perp}$ ) distributions. While no change with  $q^2$  is visible in the nucleon fragmentation or central regions, there is a fairly definite broadening<sup>44</sup> of the  $p_{\perp}$  distribution with increasing  $q^2$  in the photon fragmentation region, which is seen consistently in several experiments.

Probably the most dramatic effect seen in the data up to this time occurs in the forward charge ratio. Figure 8 shows some data on forward positive and negative hadron production for  $0.5 < q^2 < 3.0$  compared with  $\pi^-$  production for  $q^2 = 0$  at the same incident photon energy. Some, but probably not all, of the decrease of forward going  $\pi^-$ 's (and  $\pi^+$ 's) can be attributed to the rapid fall off with  $q^2$  of the  $\rho^0 p$  final state as a percentage of the total cross section.

The actual ratio of positive to negative forward-going ( $0.4 < x < 0.85$ ) hadrons is shown<sup>44, 46</sup> in Fig. 9 as a function of  $q^2$  from various experiments. The agreement of the various results for " $\gamma$ " + p collisions makes it clear that as the photon becomes more virtual, the positive charge on or within the proton is being thrown forward by the interaction. That it is not the charge on the proton that is simply "leaking" over into the photon fragmentation region (remember, we are still working at relatively low energies) comes from recent data<sup>46</sup> with the neutron as a target. Again, while the excess is smaller and the results are less statistically significant, it appears that excess positive charge is being thrown forward.<sup>47</sup> This of course cannot come from the (zero) charge on the neutron leaking over into the photon fragmentation region. It calls for an explanation in terms of the charge distribution within the neutron, and in fact is expected in some extensions of the quark parton model to include descriptions of final state hadrons. We now turn to the general theoretical discussion of final state hadron distributions to see how both the data we have been discussing in this section and various theoretical models fit in a general context.

#### IV. Some Theoretical Viewpoints on Final State Hadrons in Deep Inelastic Scattering

A great deal of effort has been expended in the past couple of years exploring the consequences of various models for deep inelastic scattering as they relate to the distribution of final state hadrons. Instead of immediately delving into these models in detail, we will first describe a rather general, essentially kinematic, classification of the various regions of rapidity available to a produced hadron. Then we will see how some specific models populate these regions and how the final state hadron distributions in different deep inelastic processes might be related.

To begin with let us recall what we might expect as the inclusive distribution of hadrons in a purely hadronic process at very high energies.<sup>48</sup> Consider, for example,  $pp \rightarrow \pi + \text{anything}$ . The form of the invariant differential cross section  $E' d\sigma/d^3p'$  expected on the basis of a model with short range correlations is indicated in Fig. 10a. At a given value of  $p'_\perp$  (which is limited) there are fragmentation regions of fixed finite length in rapidity associated with the beam and target, separated by a central plateau of constant height. Inasmuch as the total rapidity interval available is approximately of length  $\ln s$  and the fragmentation regions are of fixed finite length, we see that the central plateau is  $\ln s$  in length. The multiplicity, which for a constant total cross section is proportional to the area under the curve, then grows as the length of the central plateau grows, i.e., as  $\ln s$ .

An analogous result is to be expected for the photoproduction process  $\gamma p \rightarrow \pi + \text{anything}$ , as shown in Fig. 10b. In fact, normalizing to the total cross section, the proton fragmentation and central plateaus should be just the same as in the previous case. Only, the beam fragmentation region in Fig. 10b (of fixed, finite length in rapidity) has changed from that in Fig. 10a to one

characteristic of the photon. The question we now wish to examine in detail is: what happens when  $q^2$  varies? In particular, what happens to the length of the photon fragmentation and central regions?

To answer these questions in a rather general way we go to the standard Mueller analysis.<sup>49</sup> While this analysis, or parts of it, have previously been treated by a number of authors,<sup>50,51,52,53</sup> we will follow rather closely here the recent paper of Cahn and Colglazier.<sup>54</sup>

First consider the high energy ( $\nu$ ) behavior of the imaginary part of the forward virtual Compton amplitude. As indicated in Fig. 11, if a sum of Regge poles dominates the high energy behavior, then we can write for large  $\nu$

$$\nu \sigma_T(\nu, q^2) = \sum_i \beta_i^{\gamma\gamma}(q^2) \nu^{\alpha_i(0)} \beta_i^{NN}, \quad (56)$$

since  $\nu \sigma_T$  is proportional to the imaginary part of the forward Compton amplitude for transverse virtual photons.<sup>55</sup> If  $W_1(\nu, q^2)$  scales, then so does  $\nu \sigma_T$ , and if the Regge and scaling limits are interchangeable, we must demand the behavior

$$\beta_i^{\gamma\gamma}(q^2) \xrightarrow{q^2 \rightarrow \infty} \left(\frac{2M_N}{q^2}\right)^{\alpha_i(0)} \tilde{\beta}_i^{\gamma\gamma}. \quad (57)$$

Then at large  $\omega = 2M_N \nu / q^2$  we have

$$\nu \sigma_T = \sum_i \tilde{\beta}_i^{\gamma\gamma} \omega^{\alpha_i(0)} \beta_i^{NN}. \quad (58)$$

For  $\omega \rightarrow \infty$ , the Pommeranchuk singularity with  $\alpha(0) = 1$  should dominate so that

$$\nu \sigma_T \xrightarrow{\omega \rightarrow \infty} \tilde{\beta}_P^{\gamma\gamma} \omega \beta_P^{NN}. \quad (59)$$

Now consider the six point functions shown in Figs. 12, 13 and 14, with  $p'$  as the four-momentum of the final hadron of mass  $m$ . We define the additional variables

$$M_N^\kappa = -p \cdot p' \quad (60a)$$

$$m \nu_1 = -p' \cdot q, \quad (60b)$$

and

$$\omega_1 = 2m \nu_1 / q^2. \quad (60c)$$

Defining the nucleon fragmentation region as where  $M_N^\kappa$  is bounded (i.e., finite final hadron energies in the nucleon rest frame) as  $\nu \rightarrow \infty$ , we have in the Regge regime illustrated in Fig. 12,

$$\nu \left( \frac{E' d\sigma_T}{d^3 p'} \right) = \sum_i \beta_i^{\gamma\gamma} (q^2) \nu^{\alpha_i(0)} F_i(\kappa, p'_\perp), \quad (61)$$

as the invariant cross section  $\nu(E' d\sigma/d^3 p')$  is proportional to the imaginary part of the six point function.<sup>56</sup> The quantity  $F_i(\kappa, p'_\perp)$  describes the lower vertex in Fig. 12. In the scaling and large  $\omega$  limits Eq. (61) becomes

$$\nu \left( \frac{E' d\sigma_T}{d^3 p'} \right) = \sum_i \tilde{\beta}_i^{\gamma\gamma} \omega^{\alpha_i(0)} F_i(\kappa, p'_\perp). \quad (62)$$

As  $\omega \rightarrow \infty$ , we have using Eq. (59) for the behavior of  $\nu \sigma_T$ :

$$\frac{1}{\sigma_T} \left( \frac{E' d\sigma_T}{d^3 p'} \right) \rightarrow \frac{F_P(\kappa, p'_\perp)}{\beta_P^{NN}}. \quad (63)$$

We therefore have a prediction of "mixed" scaling:  $\frac{1}{\sigma_T} \left( \frac{E' d\sigma_T}{d^3 p'} \right)$  depends not on  $\nu$  or  $q^2$  or  $\nu$ ,  $\kappa$ , and  $p'_\perp$  separately but on  $\omega$  and on  $\kappa$  and  $p'_\perp$ . At large  $\omega$ ,

this quantity is even independent of  $\omega$ . An examination of the derivation of Eq. (63) shows that the same result would be obtained with any beam on a nucleon target. Thus  $\frac{1}{\sigma_T} (E' d\sigma/d^3p')$  should be the same in deep inelastic scattering at very large  $\omega$  as in  $\gamma N$ ,  $KN$ ,  $NN$ , etc., collisions at high energies. This result is of course just what one expects without any deep theory: at sufficiently high energy the fragments coming from the nucleon target should be independent of the incident beam.<sup>57</sup>

A similar analysis applies to the central plateau. Considering Fig. 13 in the limit of large  $\nu_1$  and large  $\kappa$ , one has the Regge expansion

$$\nu \left( \frac{E' d\sigma_T}{d^3p'} \right) = \sum_{i,j} \beta_i^{\gamma\gamma}(q^2) \nu_1^{\alpha_i(0)} f_{ij}(p'_\perp) \kappa^{\alpha_j(0)} \beta_j^{NN}. \quad (64)$$

Again proceeding to the scaling as well as large  $\omega$  and  $\omega_1 = 2m \nu_1/q^2$  limits, Eq. (64) becomes

$$\nu \left( \frac{E' d\sigma_T}{d^3p'} \right) = \sum_{i,j} \tilde{\beta}_i^{\gamma\gamma} \omega^{\alpha_i(0)} f_{ij}(p'_\perp) \kappa^{\alpha_j(0)} \beta_j^{NN} \frac{M}{m} \alpha_i(0). \quad (65)$$

Keeping only the Pommeranchuk singularity in the double limit  $\omega_1$  and  $\kappa \rightarrow \infty$ , and using the kinematic relation which holds in this regime

$$\omega \kappa \simeq \omega \sqrt{m^2 + p'_\perp{}^2} / 2M_N, \quad (66)$$

one finds

$$\frac{1}{\sigma_T} \frac{E' d\sigma_T}{d^3p'} \rightarrow \tilde{f}_{PP}(p'_\perp). \quad (67)$$

The independence of all variables except  $p'_\perp$  is equivalent to the statement that the rapidity distribution is flat. Furthermore an analysis of the derivation of

Eq. (67) shows that the same result holds for any beam or target, as is indicated by the function  $\tilde{f}_{PP}(p'_\perp)$  on the right hand side, which depends on neither the beam nor the target. Therefore we expect the same central plateau as in any purely hadronic reaction, normalized to the total cross section.

However, there is an important difference. The total rapidity interval where  $\omega_1$  and  $\kappa$  are large is of length  $\ln \omega$ , i.e., the central plateau is of length  $\ln \omega$  and not  $\ln s$ . Inasmuch as the total rapidity length available is  $\sim \ln s$ , we see that the overall current fragmentation region must be of length  $\ln s - \ln \omega \simeq \ln s \rightarrow \ln s - \ln s - \ln s/q^2 = \ln q^2$ . This important kinematic fact, although known for some time, does not seem to be widely appreciated.

Another way to see this, outside the Mueller framework, has been given by Bjorken.<sup>58</sup> Fix  $q^2$  at some large value (where scaling holds), and let  $\omega$  also be large. Now decrease  $s$  (and therefore  $\omega$ ). As  $q^2$  is fixed the current fragmentation region should also be fixed. Only the central plateau should change, i.e., decrease in length. Now for sufficiently small  $\omega$  the central plateau will have disappeared, and at that point one has total rapidity interval of length:

$$\begin{aligned} \ln s &= \ln s/q^2 + \ln q^2 \\ &\simeq \ln \omega + \ln q^2 \simeq \ln q^2 . \end{aligned}$$

Since the current fragmentation region hasn't changed in this process of decreasing  $s$ , it must occupy this length,  $\sim \ln q^2$ , at small  $\omega$ , and at large  $\omega$  as well. At large  $\omega$ , the rapidity interval  $\ln s - \ln q^2 \simeq \ln \omega$  is available for the central plateau.

We now have arrived at the most interesting and crucial question: what is the shape of  $\nu(E'd\sigma_T/d^3p')$  in the current fragmentation region. Very little can be proven. Near  $y_{\max}$ , the end of the current fragmentation region, if

multiplicities don't grow<sup>59</sup> as powers of  $q^2$ , the simplest way of satisfying the inclusive energy sum rule would be to have  $\nu(E'd\sigma_T/d^3p')$  scale in  $\omega$ . Such scaling would also allow a smooth joining of the current fragmentation region into the central plateau.<sup>54</sup>

If we assume that in the current fragmentation region  $\nu(E'd\sigma_T/d^3p')$  scales in  $\omega$ , then we may note that the kinematics demands<sup>54</sup> that  $\nu_1 \rightarrow \infty$  as  $\nu$  and  $q^2 \rightarrow \infty$  in this region. As a result in Fig. 14, the function  $F_1(q^2, \nu_1, p'_\perp)$  describing the upper vertex must actually be only a function of  $\omega_1$  and  $p'_\perp$  if it has a non-trivial limit. Therefore, as  $\omega \rightarrow \infty$  and only the Pommeranchuk singularity dominates, we have

$$\frac{1}{\sigma_T} \left( \frac{E'd\sigma_T}{d^3p'} \right) \rightarrow \tilde{F}_P(\omega_1, p'_\perp) , \quad (68)$$

so that both scaling in  $\omega$  and in  $\omega_1 = -2q \cdot p'/q^2$  occur together, i.e., we have "mixed" scaling of a special kind.

Since the analysis we have carried out is quite general, any particular model must fit into it. An interesting case is the multiperipheral model.<sup>61</sup> While the sum of ladder graphs does not scale in ordinary renormalizable theories, a suitable cut-off (say in the transverse momentum) produces a scaling result, as in the work of Drell, Levy and Yan.<sup>62</sup> Taking the imaginary part of the ladder graph and evaluating the rapidity distribution of the intermediate particles, one finds that while the central plateau is uniformly filled in the standard manner, the current fragmentation region is empty except for the single particle connected directly to the incident virtual photon, which is separated<sup>63</sup> from the other particles by a rapidity gap of length  $\ln q^2$ . The complete lack of particles in the current fragmentation region is clearly very unphysical, and any use of the multiperipheral model as a basis for extrapolating to the behavior to be actually seen experimentally in the current fragmentation region is highly suspect.

The most thoroughly investigated models for deep inelastic processes have been those involving partons. The classification of the regions of rapidity<sup>65, 66, 67</sup> in such models is shown in Fig. 15. The struck parton is found immediately after its interaction with the virtual photon near  $y_{\max}$ , and a corresponding region of finite length is labelled as the "parton fragmentation region." The position in rapidity where the struck parton was before the interaction lies at the boundary of the central plateau and current fragmentation regions and is defined as the "hole fragmentation region." Between these two regions lies a possible plateau, the "current plateau" of length  $\sim \ln q^2$ .

Let us examine the quark parton model description in some more detail starting with the parton fragmentation region. In that region the model may be implemented using the assumptions:<sup>65, 68</sup>

1. The virtual photon interacts with point, spin 1/2 constituents (the quark partons).
  2. The parton fragments into, hadrons independently of how it is produced.
  3. The hadron distribution from a given parton is only a function of  $z = p^{(\text{hadron})} / p^{(\text{parton})}$  and of  $p_{\perp}$  (of the hadron relative to the parton direction).
- The  $p_{\perp}$  distribution is assumed to be limited.

Describing the parton (type  $i$ ) fragmentation into a given hadron ( $h'$ ) by the function  $D_i^{h'}(z, p_{\perp})$ , the final hadron distribution is given by

$$\nu \left( E' \frac{d\sigma_T}{d^3p'} \right) \propto \sum_i Q_i^2 f_i(1/\omega) D_i^{h'}(z, p_{\perp}) \quad (69)$$

for  $e^+N \rightarrow e+h'+\dots$ . The variable  $z$  plays the role of the usual Feynman variable  $x$ . The same assumptions can be easily applied in inelastic neutrino reactions. Also, picturing  $e^+e^-$  annihilation into hadrons as proceeding through

production of a quark-antiquark parton pair, one has

$$\frac{E'}{\sigma} \frac{d\sigma}{d^3p'} \propto \sum_i Q_i^2 D_i^{h'}(z, p_{\perp}), \quad (70)$$

in  $e^+e^- \rightarrow h' + \dots$ . Here  $z = |\vec{p}'|/(\sqrt{|q^2|}/2)$ . Note that the assumption of limited  $p_{\perp}$  implies jets being seen at sufficiently high energies (along the parton direction of motion) on an event by event basis.

Relations among the  $D_i^{h'}$ 's allow one to relate the hadron distributions in different deep inelastic processes.<sup>68</sup> For example, conservation of isotopic spin and charge conjugation invariance imply

$$D_p^{\pi^+}(z, p_{\perp}) = D_n^{\pi^-}(z, p_{\perp}) = D_p^{\pi^-}(z, p_{\perp}) = D_p^{\pi^+}(z, p_{\perp}), \quad (71)$$

This leads directly to sum rules of the form<sup>68</sup>

$$\begin{aligned} \int_0^1 \left[ \langle n_{\pi^+} \rangle_{en} - \langle n_{\pi^-} \rangle_{en} \right] W_1^{en}(\omega) d(1/\omega) \\ = \frac{2}{7} \int_0^1 \left[ \langle n_{\pi^+} \rangle_{ep} - \langle n_{\pi^-} \rangle_{ep} \right] W_1^{ep}(\omega) d(1/\omega) \end{aligned} \quad (72)$$

for inelastic electron-nucleon scattering, and

$$\langle n_{\pi^+} \rangle = \langle n_{\pi^-} \rangle = \langle n_{\pi^0} \rangle \quad (73)$$

for  $e^+e^-$  annihilation.

Some of the data discussed in the last section on the forward charge ratio observed in electroproduction lend support for such a parton picture. Using the theory outlined above, a number of successful fits to the existing data have been made.<sup>69</sup> However, the energies as well as  $q^2$  values appropriate to the available data are not large, and no definitive test of the scaling (in  $\omega$ ) of  $\frac{E'}{\sigma} \frac{d\sigma}{d^3p'}$ , has

even been made. Nevertheless, sum rules such as Eq. (71) are certainly consistent with the data<sup>46</sup> and the model provides a simple, intuitive guide to what is seen experimentally.<sup>79</sup>

Up to this point, from the model discussed above it would appear that all the quark quantum numbers, and even quarks themselves, must appear in the parton fragmentation region. In models, such as the multiperipheral model<sup>61</sup> and early versions of the covariant parton model,<sup>63</sup> exactly this happens: there is no current plateau and the parton and its decay products are produced in isolation in rapidity as well as real space time.

Clearly at least some population of the current plateau region is necessary to escape this dilemma, i.e., a variant of the recurring question asked about the quark parton model: why don't the quarks get out? At one time it was hoped that cascade decay sequences would allow the struck parton to slow down until the fractional charge and other quark quantum numbers could be neutralized. But space-time arguments indicate that this does not work.<sup>70</sup> Instead a picture has been constructed in which  $q\bar{q}$  pairs are produced by polarization of the vacuum as the struck parton moves out of the nucleon, producing a plateau in rapidity starting at the hole fragmentation region and moving outward.<sup>67, 71</sup> An identical mechanism produces a plateau in  $e^+e^-$  annihilation. As the parton (and anti-parton) move apart, quasi-free, successive pairs are created until at a time  $\sim \sqrt{|q^2|}$  the polarization charge catches up to the parton and neutralizes it.

The result is a universal current plateau<sup>65, 67, 72</sup> in  $eN$ ,  $\nu N$ , and  $e^+e^-$  annihilation of length  $\ln q^2$  and with a constant height. Consequently the multiplicity in  $e^+e^-$  annihilation should be

$$\langle n \rangle_{e^+e^-} = C_{e^+e^-} \ln |q^2| + \text{const.} \quad (74)$$

and in eN collisions,<sup>73</sup>

$$\langle n \rangle_{en} = C_h \ln \omega + C_{e^+e^-} \ln q^2 + \text{const.} , \quad (75)$$

where  $C_h$  is the height of the hadronic central plateau.

If  $C_h = C_{e^+e^-}$ , the central and current plateaus in eN or  $\nu N$  collisions join into one of length  $\ln \omega + \ln q^2 \sim \ln s$ , as has been suggested theoretically.<sup>65, 74, 75</sup>

As a result we would have

$$\langle n_{ep} \rangle = C_h \ln s + \text{const.} \quad (76)$$

as seems suggested by a recent experiment,<sup>76</sup> although the energies involved are really too low to have seen any plateau.

With a plateau we can avoid the possibility of seeing real quarks, but are still left with the question of retention of quark quantum numbers on the average in the parton fragmentation region.<sup>65</sup> While at one time it was argued that quark quantum numbers would be "visible" in this way on general grounds, more recent work indicates that generally<sup>77, 78</sup> these quantum numbers can "leak" across the current plateau. This is particularly transparent in a model of  $e^+e^-$  annihilation where quarks and antiquarks are paired so that only mesons populate the final state<sup>77</sup> — there is no chance of observing fractional baryon number in such a case. Still, the measurement of average quantum numbers in the parton fragmentation region is of some interest,<sup>79</sup> it being one of the few places where traces of quarks might be seen even in the absence of the real thing.

Critical tests of at least parts of this picture may come quite soon. The parton fragmentation region and even the current plateau should be accessible with the generation of  $e^+e^-$  rings now built or being built. However, to see the full glory of the "limosine" in Fig. 15 will take some time. To see both the

central and current plateaus clearly, our experience with hadrons indicates one would like  $\ln \omega \gtrsim 6$  and  $\ln q^2 \gtrsim 6$ , or  $\ln s \gtrsim 12$ ! For the moment we will have to content ourselves with viewing pieces<sup>80</sup> of the Volkswagen in Fig. 16.

## REFERENCES

1. We use a metric where  $p \cdot p = \vec{p}^2 - p_0^2$ , so that  $q^2 > 0$  for space-like four-vectors  $q_\mu$ . The fine structure constant  $\alpha = e^2/4\pi \approx 1/137$ .
2. F.J. Gilman, Phys. Reports 4 C, 98 (1972) reviews the kinematics of inelastic scattering, scaling and the parton model. See the references to previous work therein.
3. R.L. Jaffe, Phys. Rev. D 6, 716 (1972) treats the effect of singularities elsewhere in coordinate space.
4. H. Fritzsch and M. Gell-Mann, in Scale Invariance and the Light Cone (Gordon and Breach, New York, 1971), Vol. 2, p. 1.
5. Y. Frishman, in Proceedings of the XVI International Conference on High Energy Physics, J.D. Jackson and A. Roberts, editors (National Accelerator Laboratory, Batavia, Illinois, 1972), p. 119, reviews the subject of light cone and short distance singularities. See references to previous work therein.
6. M. Gell-Mann, Phys. Rev. 125, 1067 (1962).
7. J.D. Bjorken, Phys. Rev. 179, 1547 (1969).
8. R.P. Feynman, Phys. Rev. Letters 23, 1415 (1969).
9. J.D. Bjorken and E.A. Paschos, Phys. Rev. 185, 1975 (1969).
10. M. Breidenbach, et al., Phys. Rev. Letters 23, 935 (1969);  
E.D. Bloom, et al., Phys. Rev. Letters 23, 930 (1969).
11. G. Miller, et al., Phys. Rev. D 5, 528 (1972).
12. E.M. Riordan, MIT thesis, 1973 (unpublished).
13. E.D. Bloom, et al., Stanford Linear Accelerator Center Report No. SLAC-PUB-796 presented to the XV International Conference on High Energy Physics, Kiev, USSR, 1970 (unpublished).

14. A. Bodek, *et al.*, Phys. Rev. Letters 30, 1087 (1973).
15. O. Nachtman, Nucl. Phys. B 38, 397 (1972).
16. E.D. Bloom, invited talk presented at the International Conference on New Results from Experiments on High Energy Particle Collisions, Vanderbilt University, Nashville, March 26-28, 1973 and Caltech preprint CALT-68-392, 1973 (unpublished).
17. K. Gottfried, Phys. Rev. Letters 18, 1174 (1967).
18. P.M. Fishbane and D.Z. Freedman, Phys. Rev. D 5, 2582 (1972).
19. C.H. Llewellyn Smith, Physics Reports 3C, 261 (1972), reviews the general subject of neutrino reactions. See references to previous work therein.
20. S.L. Adler, Phys. Rev. 143, 1144 (1966).
21. D.J. Gross and C.H. Llewellyn Smith, Nucl. Phys. B 14, 337 (1969).
22. D.H. Perkins, in Proceedings of the XVI International Conference on High Energy Physics, J.D. Jackson and A. Roberts, editors (National Accelerator Laboratory, Batavia, 1972), Vol. 4, p. 189, reviews the data and related phenomenology on the basis of the Gargamelle experiment. See references therein.
23. The same result is also obtainable by assuming that the isoscalar electromagnetic current is responsible for 10% of  $F_2^{ep}(x) + F_2^{en}(x)$  and there are equal vector and axial-vector contributions to  $F_2^{\nu N}(x)$  or  $F_2^{\bar{\nu} N}(x)$ . See D.H. Perkins, Ref. 78.
24. A more careful treatment makes (small) corrections for the non-zero value of the Cabibbo angle and for the excess of target neutrons over protons in nuclei. See D.H. Perkins, Ref. 78.

25. Correction for the excess of target neutrons over protons in nuclei yields  $B = 0.86 \pm 0.04$ . See D.H. Perkins, Ref. 78.
26. B.C. Barish, et al., Phys. Rev. Letters 31, 565 (1973).
27. A. Benvenuti, et al., Phys. Rev. Letters 30, 1084 (1973).
28. D. Cline, invited talk at the Stanford Linear Accelerator Center Summer Institute in Particle Physics, July, 1973 (unpublished) and references therein.
29. J.D. Bjorken, D. Cline and A.K. Mann, Stanford Linear Accelerator Center Report No. SLAC-PUB-1244, 1973 (unpublished).
30. W.A. Bardeen, H. Fritzsch, and M. Gell-Mann, in Proceedings of the Topical Meeting on Conformal Invariance in Hadron Physics, Frascati, May, 1972 (unpublished).
31. M. Han and Y. Nambu, Phys. Rev. 139, 1006 (1965).
32. R.F. Schwitters, invited talk at the Stanford Linear Accelerator Center Summer Institute on Particle Physics, July, 1973 (unpublished) and references therein.
33. H.B. Newman, invited talk at the Stanford Linear Accelerator Center Summer Institute in Particle Physics, July, 1973 (unpublished) and references therein.
34. M.S. Chanowitz and S.D. Drell, Phys. Rev. Letters 30, 807 (1973).
35. E.D. Bloom, invited talk at the VI International Symposium on Electron and Photon Interactions at High Energy, Bonn, August, 1973 (unpublished).
36. D.J. Gross, invited talk at the Stanford Linear Accelerator Center Summer Institute on Particle Physics, July, 1973 (unpublished) and references therein.
37. See, for example, the talk of K. Berkelman, in Proceedings of the XVI

International Conference on High Energy Physics, J.D. Jackson and

A. Roberts, editors (National Accelerator Laboratory, Batavia, 1972),

Vol. 4, p. 41.

38. J.T. Dakin, et al., Phys. Rev. Letters 30, 142 (1973). See also M. Perl, lectures at the Stanford Linear Accelerator Center Summer Institute on Particle Physics, July, 1973 (unpublished) for a review of the data on final state hadrons and references therein.
39. K. Berkelman, invited talk at the Stanford Linear Accelerator Center Summer Institute on Particle Physics, July, 1973 (unpublished) and L. Ahrens et al., Phys. Rev. Letters 31, 131 (1973).
40. V. Eckardt, et al., DESY preprint, 1973 (unpublished) presents results on  $\rho$  and  $\omega$  production.
41. J. Ballam, et al., Stanford Linear Accelerator Center report no. SLAC-PUB-1163, 1972 (unpublished); and J.T. Carroll, invited talk at the Stanford Linear Accelerator Center Summer Institute on Particle Physics, July, 1973 (unpublished).
42. J. Ballam, et al., Phys. Rev. D 5, 545 (1972).
43. V. Eckardt, et al., DESY preprint, 1973 (unpublished) presents results on inclusive cross sections.
44. G.J. Feldman, invited talk at the Stanford Linear Accelerator Center Summer Institute on Particle Physics, July, 1973 (unpublished) reviews the inclusive data and contains references thereto.
45. J.T. Dakin, et al., Phys. Rev. Letters 29, 746 (1972).
46. J.T. Dakin, et al., Stanford Linear Accelerator Center report no. SLAC-PUB-1269, 1973 (unpublished).

47. Recent data of C.J. Bebek, et al., Harvard preprint submitted to the Bonn Conference, 1973 (unpublished) show a ratio of positive to negative forward hadrons which is less than one with a neutron target. Strictly speaking there is no contradiction as these data are in a different kinematic range (smaller  $\nu$  and  $\omega$ ) than those of Ref. 46, but further high statistics data are needed to resolve the  $\nu$  and  $q^2$  dependence.
48. See, for example, M. Jacob, lectures in these proceedings.
49. A. Mueller, Phys. Rev. D 2, 2963 (1970).
50. S. R. Choudhury and R. Rajaraman, Phys. Rev. D 2, 2963 (1970).
51. H.D.I. Arbaranel and D.J. Gross, Phys. Rev. D 5, 699 (1972).
52. K. Bardakci and N. Pak, Lettere al Nuovo Cimento 4, 719 (1972); see also N. Pak, Ph.D. Thesis, University of California, Berkeley, 1972 (unpublished).
53. J. Cleymans, Stanford Linear Accelerator Center report no. SLAC-PUB-1119, 1972 (unpublished).
54. R.N. Cahn and E.W. Colglazier, Stanford Linear Accelerator Center report no. SLAC-PUB-1194, 1973 (unpublished).
55. While we always deal with the transverse cross sections,  $\sigma_T$  or  $d\sigma_T/d^3p'$ , completely analogous formulas can be written for the longitudinal cross sections by a trivial change of subscripts.
56. We will always be considering cross sections averaged over the azimuthal angle,  $\phi$ , so that the second and fourth terms in Eq. (54) vanish.
57. This has also been derived in Refs. 50-54 and by J. Ellis, Phys. Letters 35B, 537 (1971); J. Stack, Phys. Rev. Letters 28, 57 (1972); and A. Schwimmer, Phys. Rev. D 8, 974 (1973) in the light cone framework, and by S. Drell and T.M. Yan, Phys. Rev. Letters 24, 855 (1970) in a parton picture. See also Ref. 63.

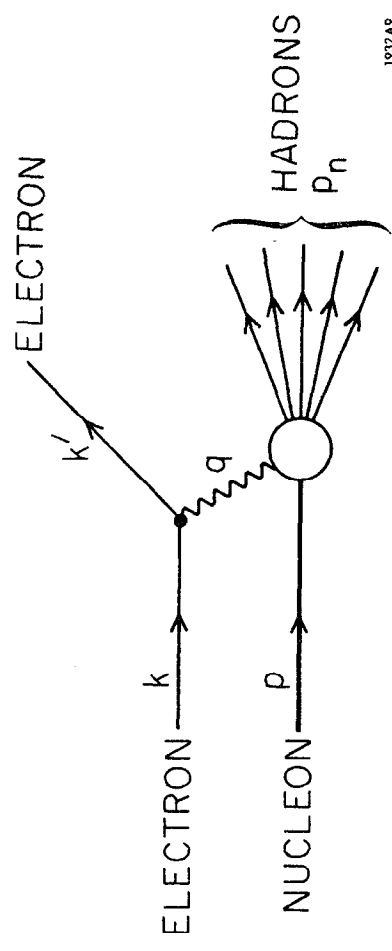
58. J.D. Bjorken, in Proceedings of the 1971 International Symposium on Electron and Photon Interactions at High Energies, N.B. Mistry, editor (Laboratory of Nuclear Studies, Cornell, 1972), p.281.
59. Such a growth of the multiplicity is found in the "pulverization" model of T.T. Chou and C.N. Yang, Phys. Rev. D 4, 2005 (1971). See also R.C. Hwa and C.S. Lam, Phys. Rev. D 4, 2865 (1971); H.J. Nieh and J.M. Wang, Phys. Rev. Letters 26, 1139 (1971); and C. Quigg and J. M. Wang, Phys. Rev. D 6, 2690 (1972). Another model which lacks scaling (in  $\omega$ ) of  $\frac{1}{\sigma_T} (E' d\sigma_T/d^3p')$  is the dual model as examined by M.A. Gonzalez and J.H. Weis, University of Washington preprint, 1973 (unpublished).
60. E. Predazzi and G. Veneziano, Nuovo Cimento Letters 2, 749 (1971).
61. See, for example, H.D.I. Abarbanel, M.L. Goldberger and S.B. Treiman, Phys. Rev. Letters 22, 500 (1969); G. Altarelli and H. Rubinstein, Phys. Rev. 187, 2111 (1969); J.D. Dorren, Nucl. Phys. B 36, 541 (1972); and S.S. Shei and D.M. Tow, Phys. Rev. D 4, 2056 (1971).
62. S.D. Drell, D.J. Levy and T.M. Yan, Phys. Rev. 187, 2159 (1969) and *ibid.*, D 1, 1035, 1617, 2412 (1970).
63. A similar phenomenon occurs in the earlier versions of the covariant parton model: see P.V. Landshoff and J.C. Polkinghorne, Nucl. Phys. B 33, 221 (1971) and Phys. Reports 5 C, 1 (1972) and references therein.
64. See also G. Altarelli and L. Maiani, Nucl. Phys. B 56, 477 (1973).
65. R.P. Feynman, Photon-Hadron Interactions (W.A. Benjamin, Reading, Mass., 1972).
66. J.D. Bjorken, Phys. Rev. D 7, 282 (1973).
67. See J.D. Bjorken, lectures at the Stanford Linear Accelerator Center Summer Institute on Particle Physics, July, 1973 (unpublished) and references therein.

68. M. Gronau, F. Ravndal and Y. Zarmi, Nucl. Phys. B 51, 611 (1973)  
implement the quark parton model in the parton fragmentation region in  
detail.
69. Fits have been made along these lines by J. Cleymans and R. Rodenberg,  
Aachen preprint, 1973 (unpublished); J.T. Dakin and G.J. Feldman,  
Stanford Linear Accelerator Center report no. SLAC-PUB-1273, 1973  
(unpublished); and P. Hasenfratz, Budapest preprint no. KFKI-73-1,  
1973 (unpublished).
70. J. Kogut, D.K. Sinclair and L. Susskind, Phys. Rev. D 7, 3637 (1973).
71. Such a picture is realized in one dimensional electrodynamics; see  
A. Casher, J. Kogut and L. Susskind, Tel Aviv University preprint no.  
373-73, 1973 (unpublished).
72. Such a plateau has also been found in the massive quark model: see,  
G. Preparata, Phys. Rev. D 7, 2973 (1973) and R. Gatto and G. Preparata,  
DESY preprint no. 73/15, 1973 (unpublished); and in the covariant parton  
model: R. L. Kingsley, et al., Cambridge preprint no. DAMTP 73/19,  
1973 (unpublished).
73. R.N. Cahn, J.W. Cleymans and E.W. Colglazier, Phys. Letters 43 B,  
323 (1973).
74. J.D. Bjorken and J. Kogut, Stanford Linear Accelerator Center report no.  
SLAC-PUB-1213, 1973 (unpublished).
75. J. Kogut, Institute for Advanced Study, preprint no. COO-2220-12, 1973  
(unpublished).
76. K. Berkdman, et al., Cornell preprint no. CLNS-240, submitted to the  
Bonn Conference, 1973 (unpublished).
77. G.R. Farrar and J.L. Rosner, Phys. Rev. D 7, 2747 (1973).

78. R.N. Cahn and E.W. Colglazier, Stanford Linear Accelerator Center report no. SLAC-PUB-1267, 1973 (unpublished).
79. See the discussion of testing for quark quantum numbers in E.W. Colglazier, invited talk at the Stanford Linear Accelerator Center Summer Institute on Particle Physics, July, 1973 (unpublished). See references to other work on the current fragmentation region therein.
80. I thank Drs. R.N. Cahn, E.W. Colglazier and J. Ellis for this analogy and many discussions.

## FIGURE CAPTIONS

1. Kinematics of inelastic electron-nucleon scattering.
2. The structure functions  $\nu W_2$  and  $2M_N W_1$  versus  $\omega'$  for various  $q^2$  ranges.<sup>11</sup>
3. The ratio of neutron to proton inelastic electron scattering cross sections<sup>16</sup> for large values of  $\omega'$ .
4. The x distribution of inelastic neutrino scattering from the Caltech experiment<sup>26</sup> at NAL compared to  $F_2^{\text{ed}}(x)$  measured at SLAC.
5. Values of  $\langle q^2 \rangle$  plotted versus the incident neutrino energy, E, from the Caltech experiment<sup>26</sup> at NAL.
6. Experimental results<sup>32</sup> for  $\sigma(e^+e^- \rightarrow \text{hadrons})/\sigma(e^+e^- \rightarrow \mu^+\mu^-)$ .
7. The ratio<sup>38</sup> of the rho production cross section to the total cross section as a function of  $q^2$ .
8. The invariant cross section for the inclusive production<sup>45</sup> of positive and negative hadrons on protons near the forward direction for  $0.5 \text{ GeV}^2 < q^2 < 3.0 \text{ GeV}^2$  and  $\pi^-$  production for  $q^2 = 0$  versus the Feynman variable x.
9. The ratio of positive to negative hadrons in the range  $0.4 < x < 0.85$  on proton and neutron targets as a function of  $q^2$ .
10. Schematic rapidity distributions of pions produced in the reactions: (a)  $pp \rightarrow \pi + \text{anything}$  and (b)  $\gamma p \rightarrow \pi + \text{anything}$ .
11. Regge pole exchanges in high energy forward Compton scattering.
12. Mueller Regge six-point function relevant to the nucleon fragmentation region.
13. Mueller Regge six-point function relevant to the central plateau.
14. Mueller Regge six-point function relevant to the current fragmentation region.
15. The five regions of rapidity for inclusive hadron production in the parton model at large  $\omega$  and  $q^2$ .
16. A possible rapidity distribution in the parton model at energies available in the foreseeable future.



1932A9

Fig. 1

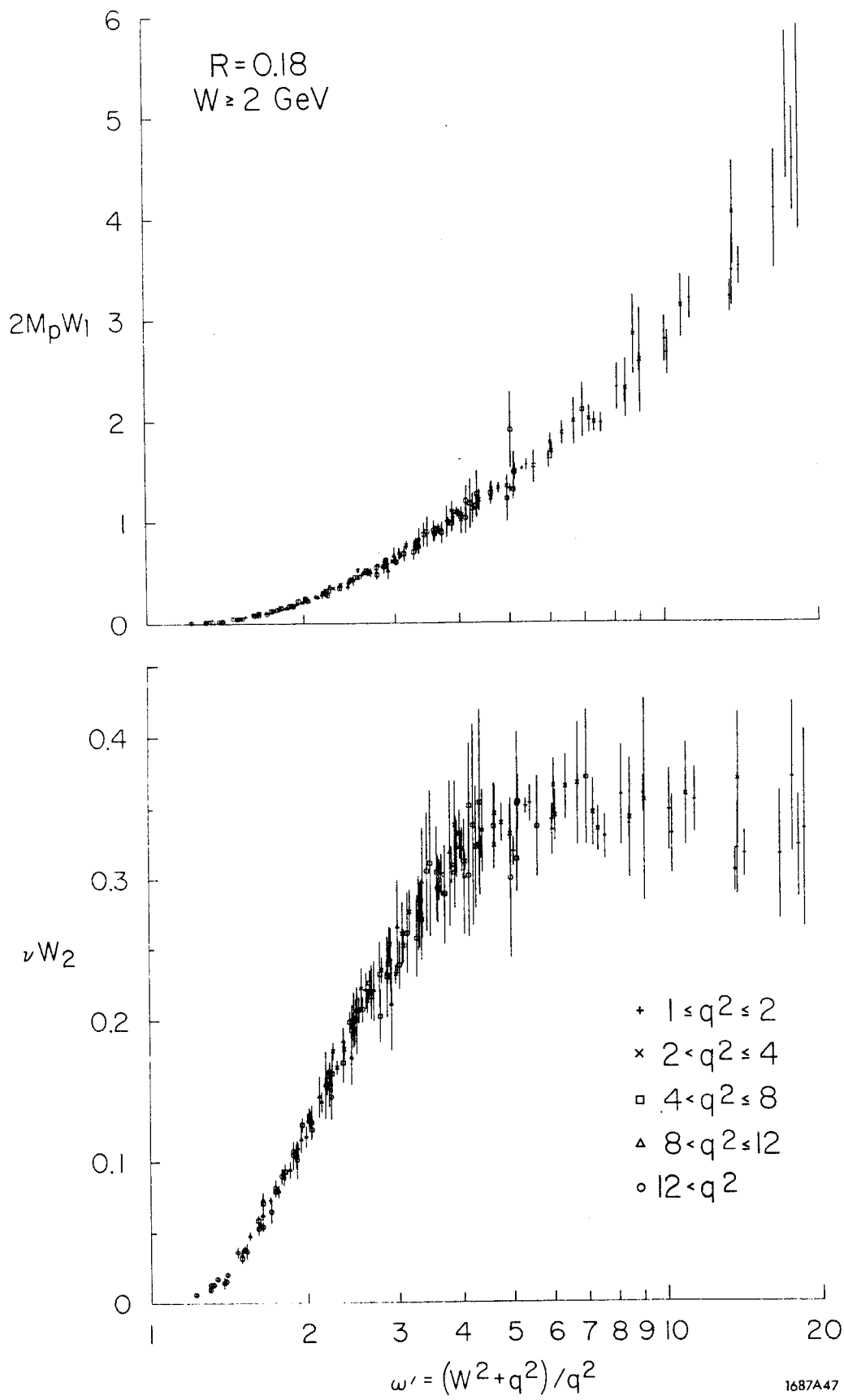


Fig. 2

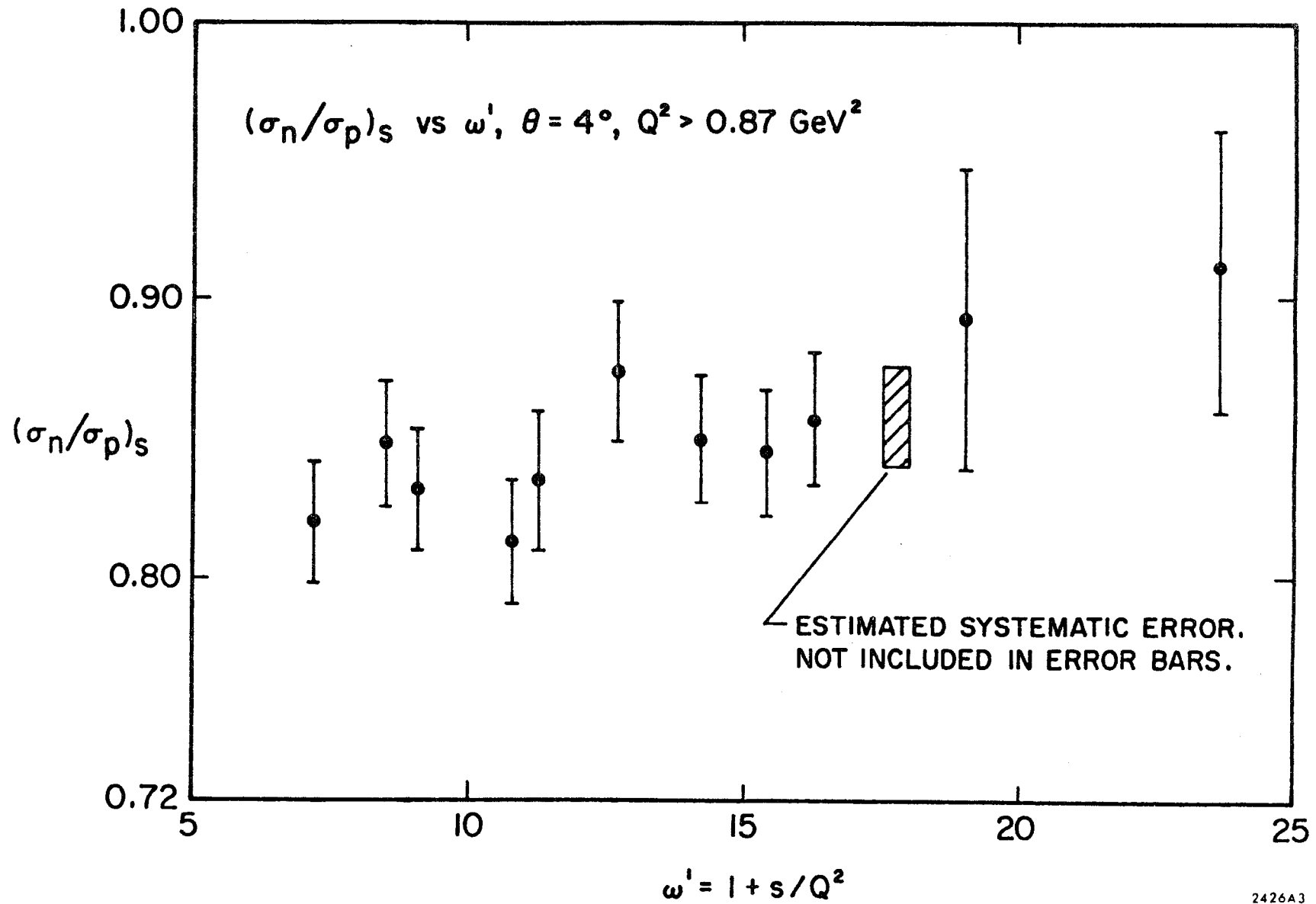


Fig. 3

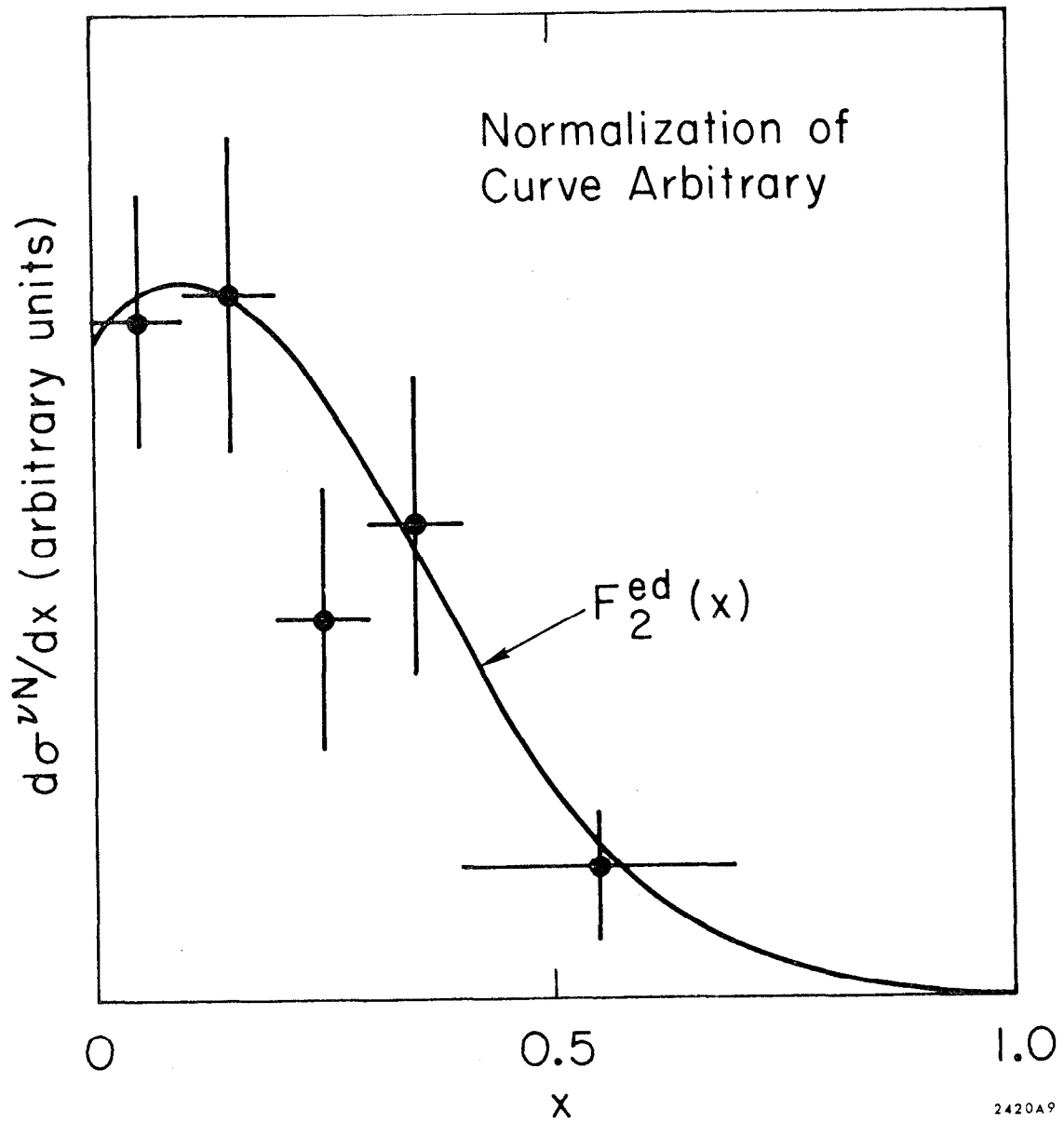


Fig. 4

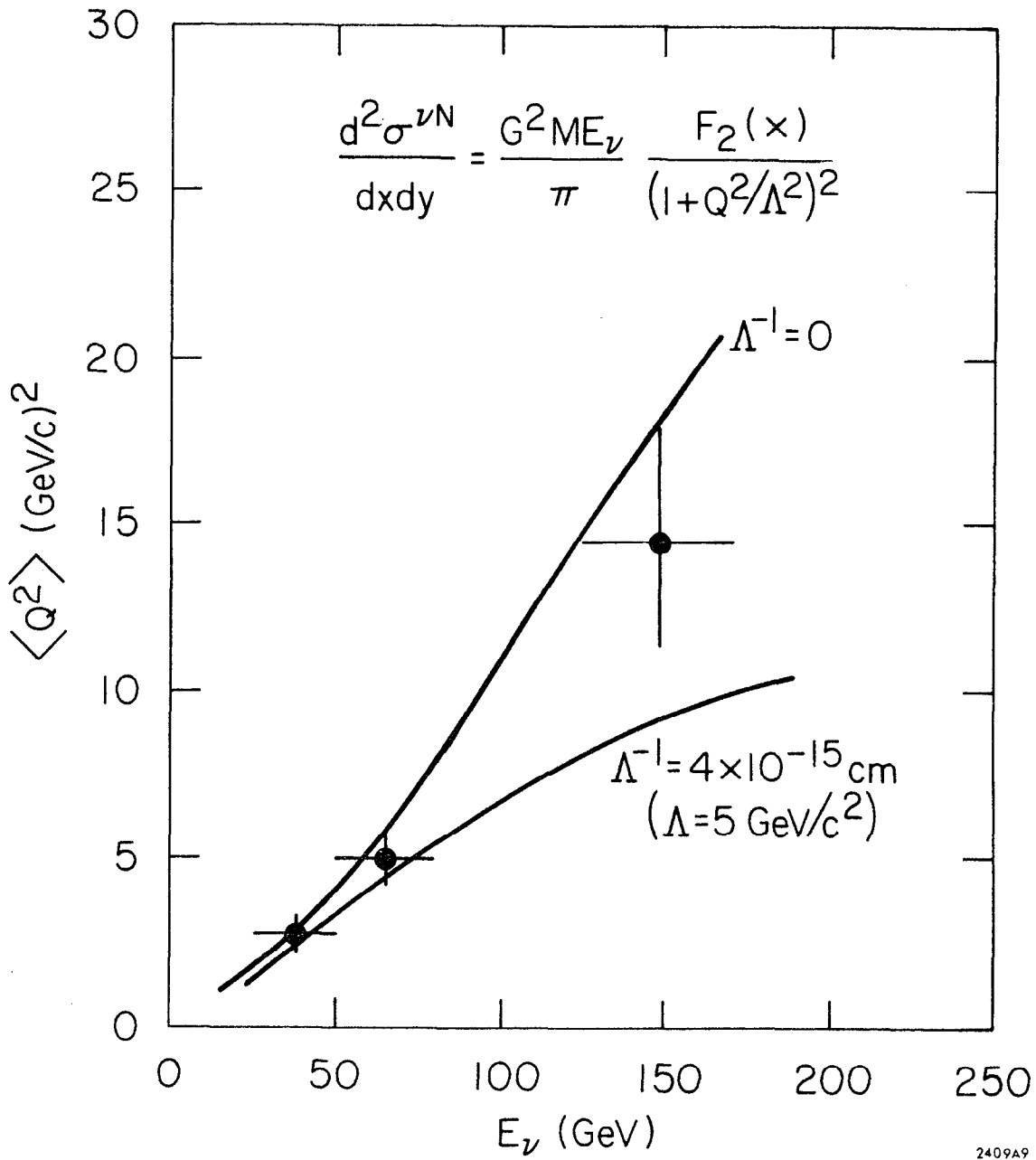


Fig. 5

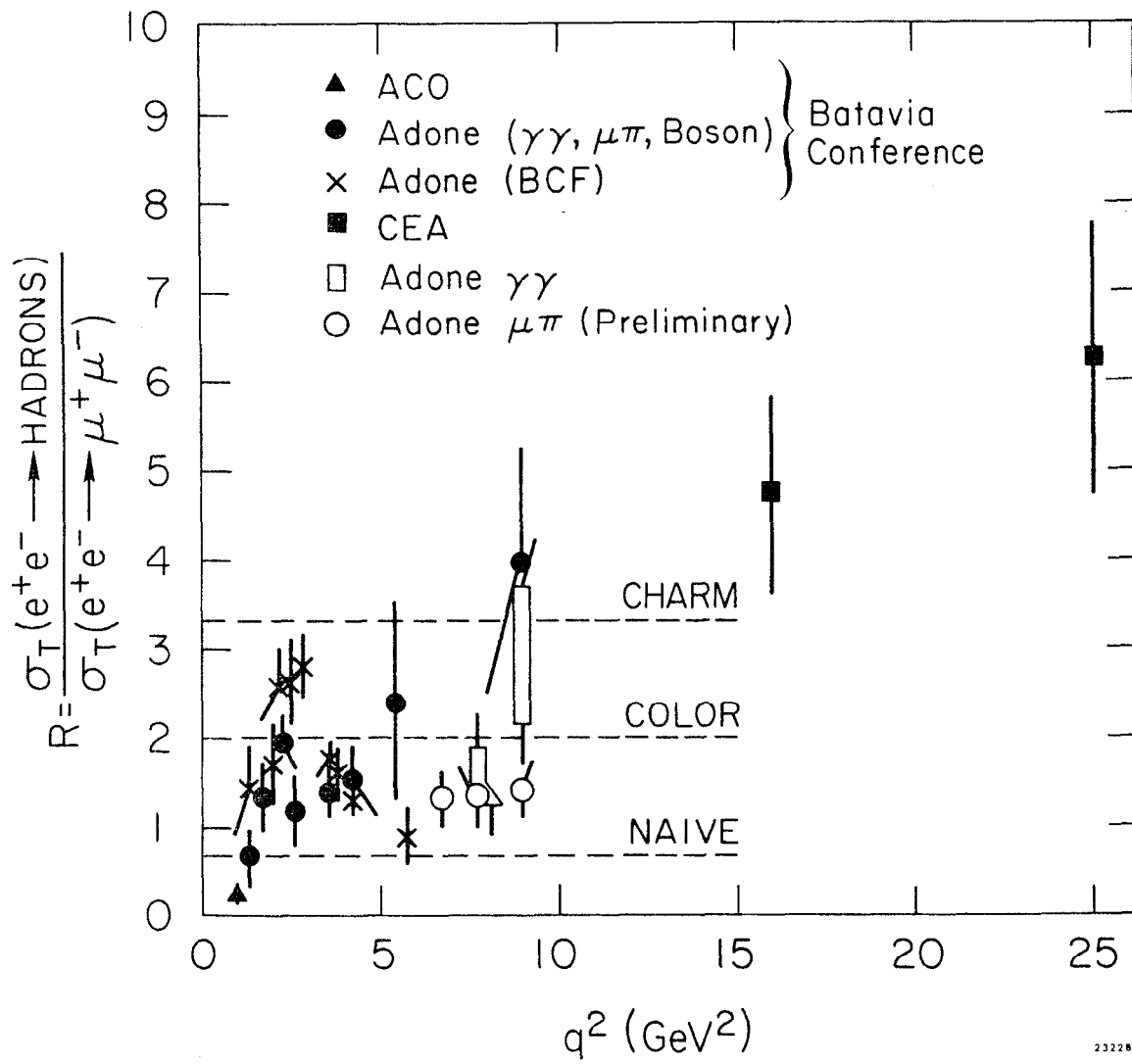


Fig. 6

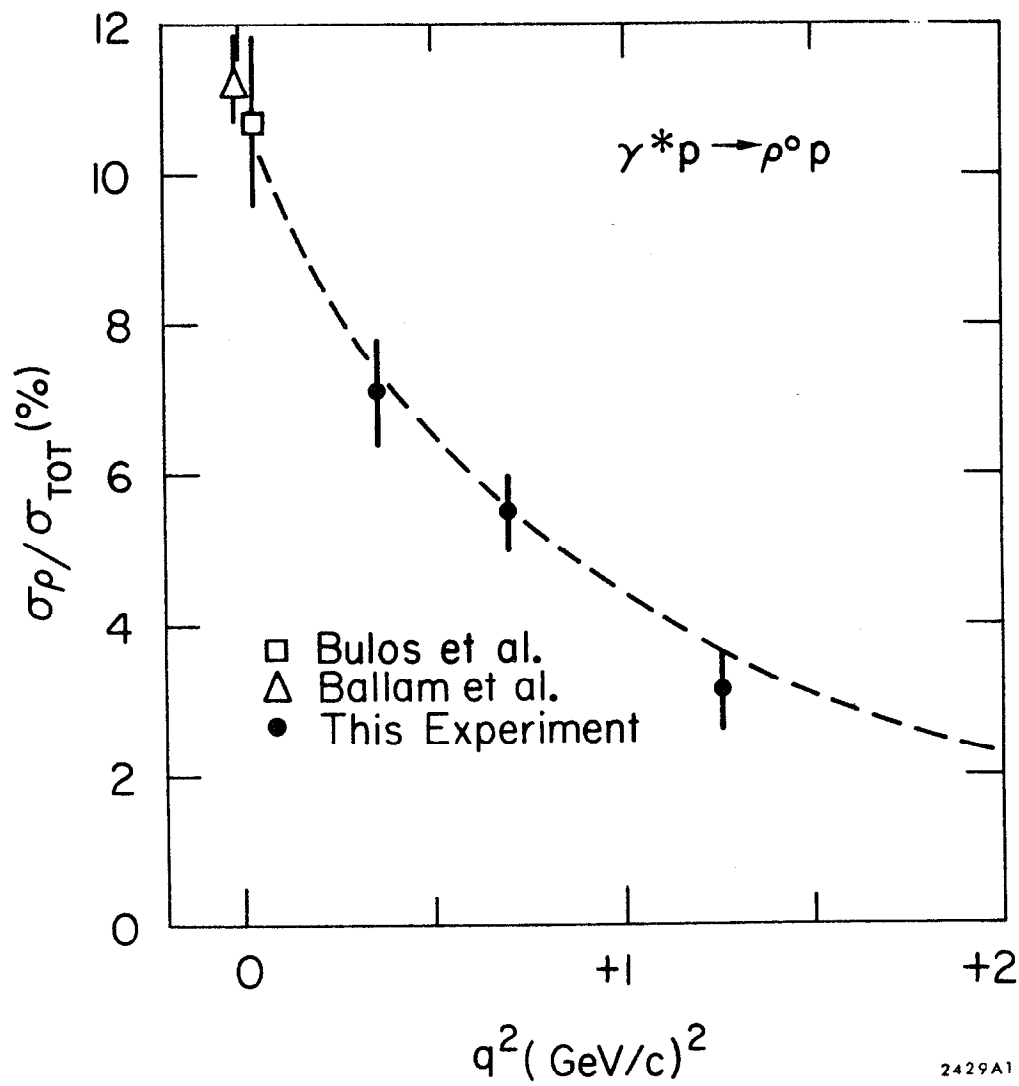


Fig. 7

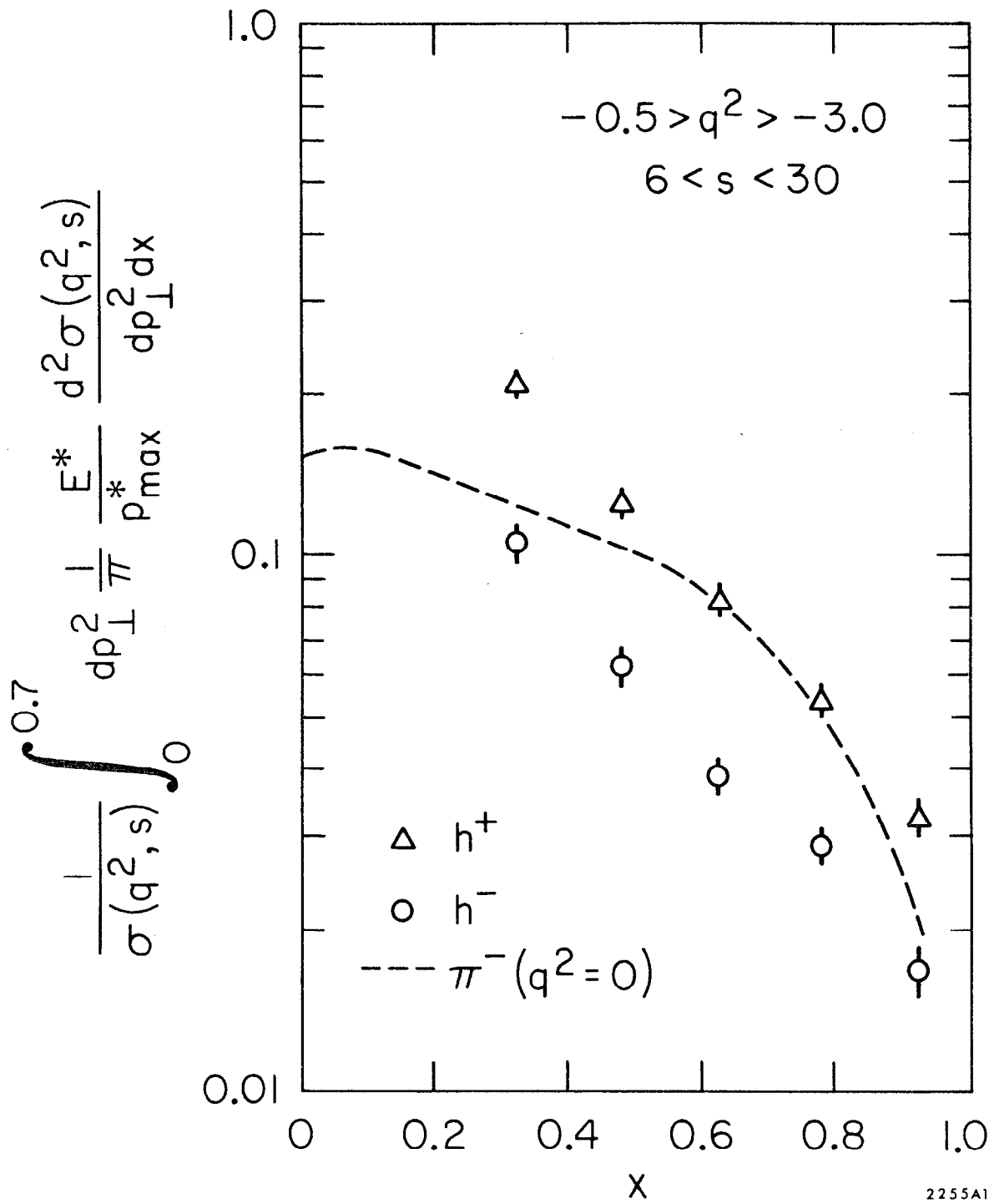
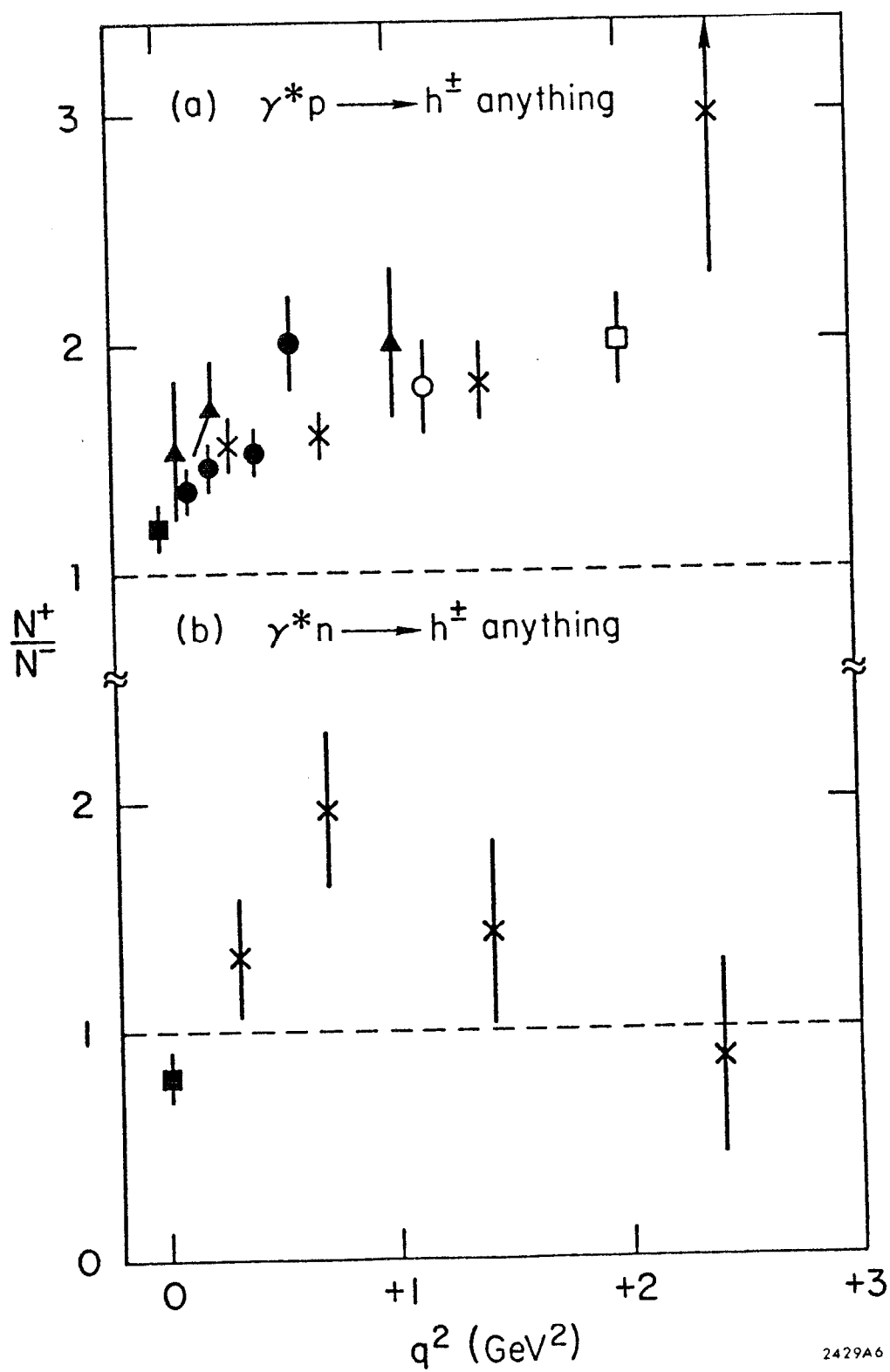


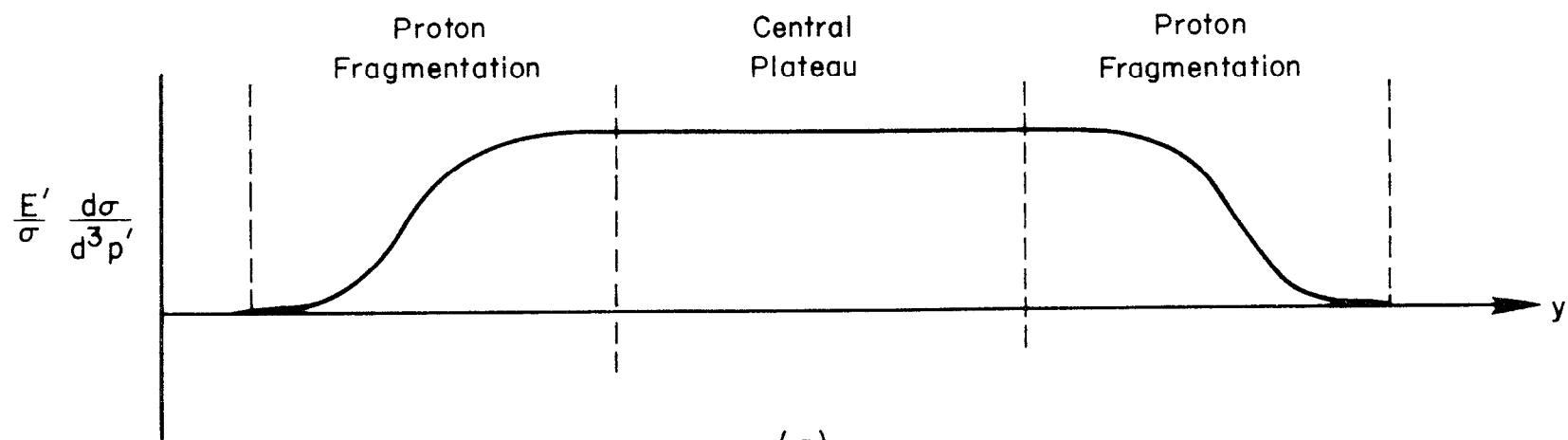
Fig. 8

- |   |                 |   |               |
|---|-----------------|---|---------------|
| × | This Experiment | ○ | Alder et al.  |
| ■ | Gandsman et al. | □ | Bebek et al.  |
| ● | Dammann et al.  | ▲ | Ballam et al. |

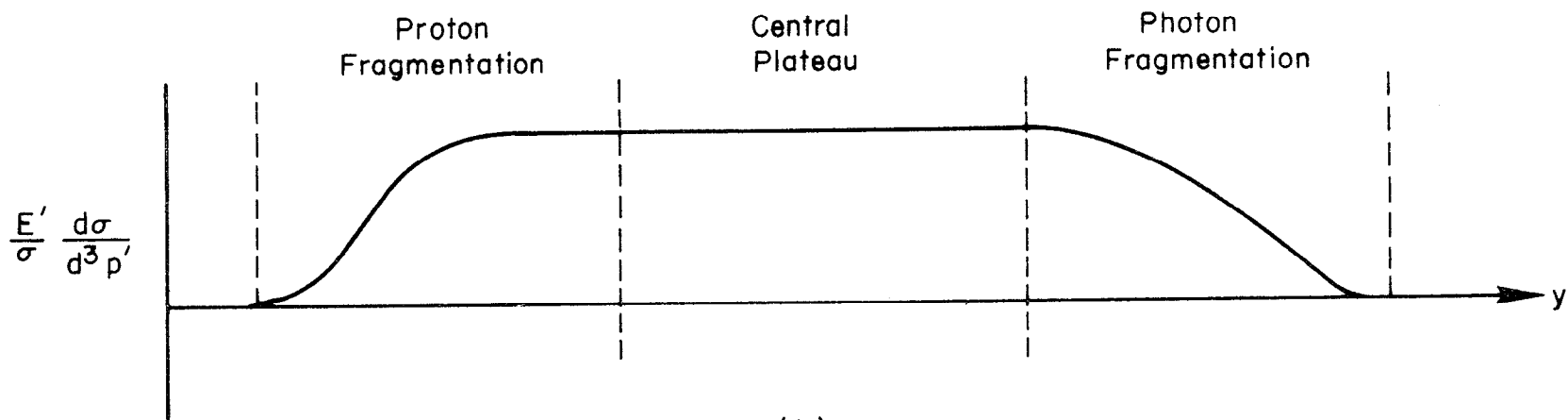


2429A6

Fig. 9



(a)



(b)

2429A7

Fig. 10

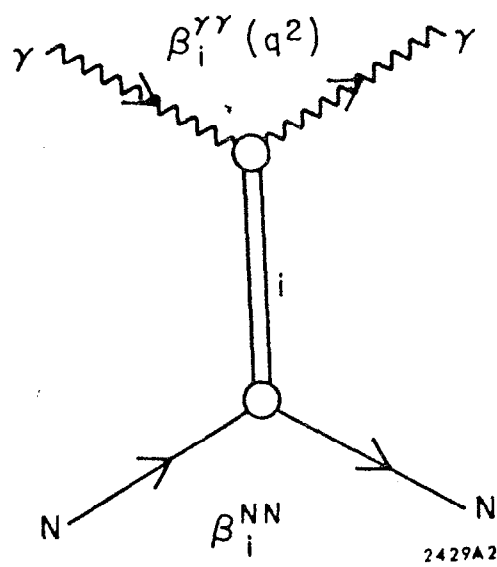


Fig. 11

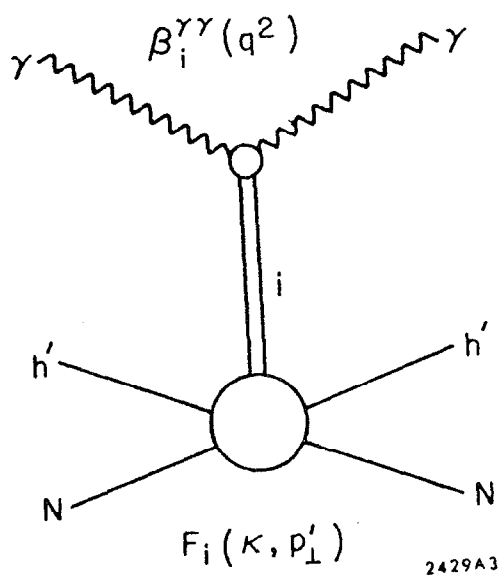


Fig. 12

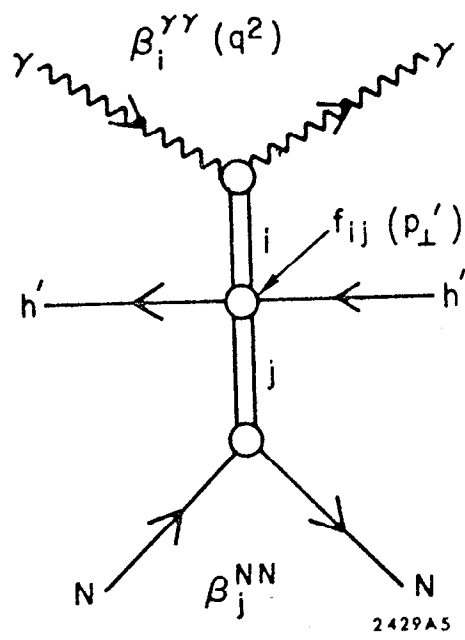


Fig. 13

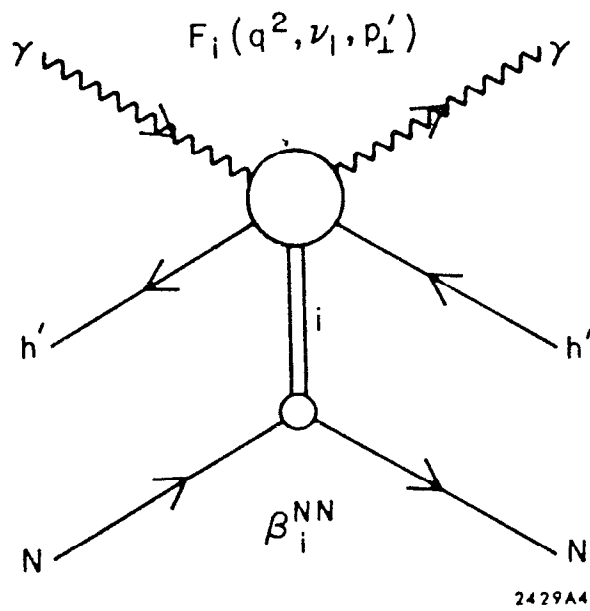
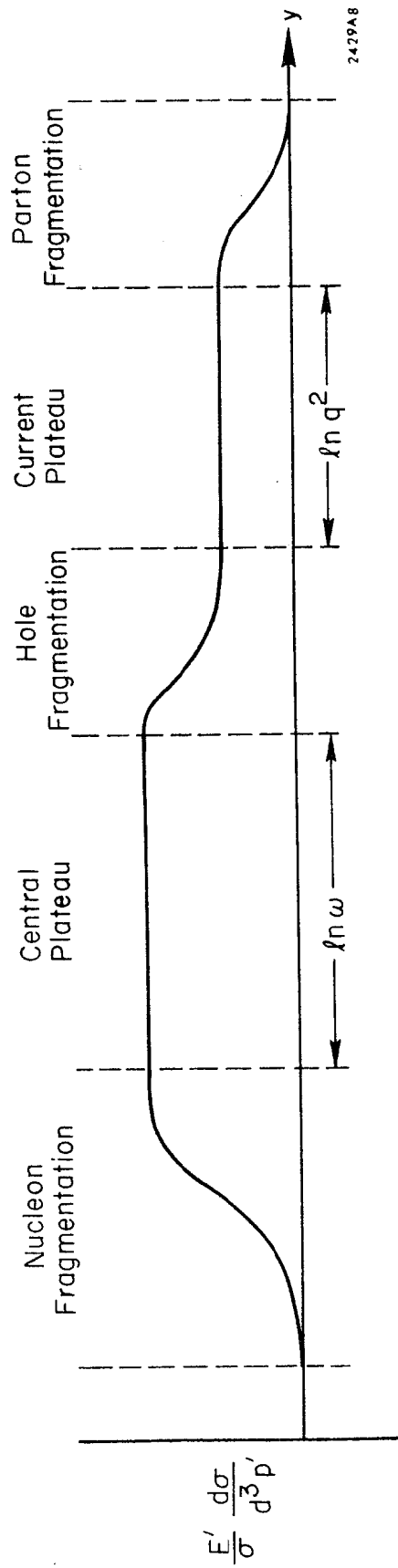
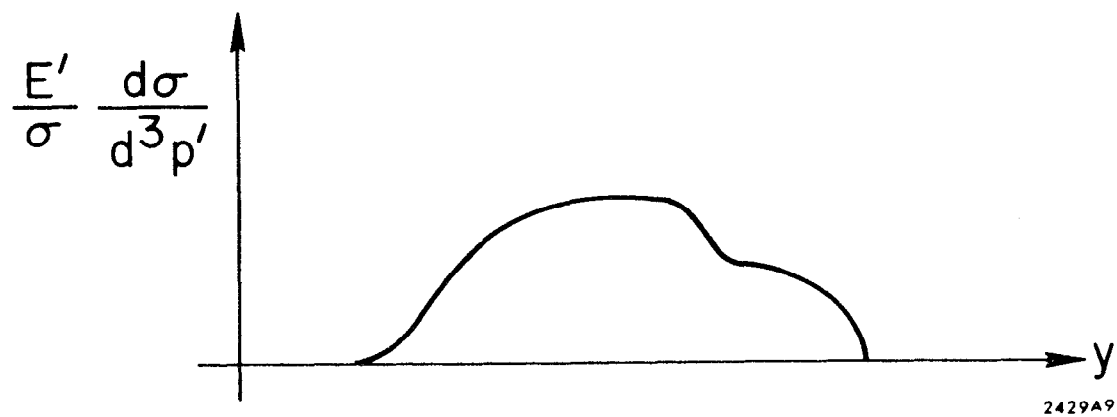


Fig. 14



2429A8

Fig. 15



2429A9

Fig 16